



Asian Journal of Pharmaceutical Analysis and Medicinal Chemistry

Journal home page: www.ajpamc.com

<https://doi.org/10.36673/AJPAMC.2020.v08.i04.A19>



VIRTUAL SCREENING, MOLECULAR DOCKING, PHARMACOKINETIC, PHYSICO-CHEMICAL AND MEDICINAL PROPERTIES OF POTENTIAL CURCUMIN DERIVATIVES AGAINST SARS-CoV-2 MAIN PROTEASE (Mpro)

Abhishek Kumar Verma^{1a}, Habiba Ali Bala², Isyaku Ibrahim Muhammad², Adamu Muhammad²,
Abhay Raj Kori³, Mayadhar Barik*

^{1a}Assistant Professor, Department of Life Sciences, Faculty of Science and Technology, Mewar University, Gangrar, Chittorgarh, Rajasthan, India.

²Department of Life Sciences, Faculty of Sciences & Technology, Mewar University, Chittorgarh, Rajasthan, India.

³Research Scholar, Department of Zoology, University of Allahabad, Allahabad, India.

ABSTRACT

Coronaviruses are one of the transmissible viruses that are mostly reliable for respiratory, intestinal and urogenital tract infections. Various researchers demonstrated that the main protease (MPRO) protein might be an important drug target for SARS-CoV-2. The treatment of illnesses by the oral tradition have long been associated with Natural herbal remedies (NHRs). Modern medicine has potential effects, thanks to traditional medicine, the effectiveness of which derives from medicinal plants including with herbs and shrubs. Objective of this study is to confirm the ingredient of the natural origin compounds (NOCs) which have a potential of anti-viral effect (AVE) and can prevent the humans from SARS-CoV-2 infection. We are interested to figure out the interaction study between the molecules of natural origin compound and the protein of SARS-CoV-2 through molecular docking. The inhibition of Coronavirus (nCoV-2019) main protease enzyme is an important target of our study. All the compounds from *Curcuma longa L.* (Zingiberaceae family) had been screened for the inhibition of MPRO protein through *in silico* methods. From molecular docking report the results we obtained that is out of 235 molecules of natural origin the derivative of Curcumin are one of the best compounds determined through molecular docking and hydrogen bonding with interaction are proposed as the may be novel inhibitor for the SARS-CoV-2 main protease. We demonstrate using Swiss ADME online server tools that all sixteen molecules have better “drug-likeness” than control and does not violate any Ghose, Lipinski, Egan, Veber or Muegge rules. Importantly, all sixteen compounds may be more potent than chloroquine in treatment of COVID-19 according to Molecular docking, interactions and ADME Properties.

KEYWORDS

Molecular docking, ADME properties, *Curcuma longa L.*, Inhibitor, Main protease, SARS-CoV-2.

Author for Correspondence:

Mayadhar Barik, (Sir Apj Abdul Kalam & Tejaswini Awardee),
Chief Researcher Basic and Clinical Sciences under Science and
Technology Division and Associate Professor, Mewar University,
Gangrar, Chittorgarh, Rajasthan-312901, India.

Email: mayadharbarik@gmail.com

INTRODUCTION

Coronaviruses are a type of RNA viruses that causes respiratory, intestinal and urogenital tract infection in birds and mammals. These SARS-CoV-2 contains positive-sense non segmented single-stranded RNA that are member of family Coronaviridae, subfamily

Orthocoronavirinae, order *Nidovirales*, and realm *Riboviria*^{1,2}. They are classified in four genera- Alpha coronavirus (Human coronavirus 229E, Human coronavirus NL63), Beta coronavirus (Severe acute respiratory syndrome-related coronavirus SARS-CoV-2, Tylonycteris bat coronavirus HKU4), Gamma coronavirus (Avian coronavirus, Beluga whale coronavirus SW1) and Delta coronavirus (Bulbul coronavirus HKU11, Porcine coronavirus HKU15)³⁻⁶.

Recently it has been reported that the virus might have entered the human body system as their intermediate host by binding with the ACE-2 Receptor (Angiotensin Converting Enzyme-2 Receptor) of the cell located in the lung. The single stranded and short-segmented coronaviruses have the unique pattern of the genetic material^{7,8}. The function of both the [genome and messenger RNA (m-RNA)] encoded as nonstructural protein 5 (Nsp5)⁹⁻¹¹. The Nsp5 nonstructural protein has three unique domains basically D1, D2 and D3. Among them D1 and D2 domain takes part into the 3-chymotrypsin like protease activity (3CLpro) that control coronavirus replication. Researchers characterized that Mpro that is 3CLpro of nonstructural protein is one of the promising drug targets for SARS-CoV2. The 3C-like protease enzyme Mpro is able to cleave at the carboxy terminus of a larger group of coronavirus replicase poly protein 1ab¹².

Auto cleavage of NSP 5 protein resulted product with the 3-chymotrypsin like 2 (3CLpro) enzyme having the catalytic activity and helps to dissociate and form the Nsp4-Nsp16 proteins¹⁰. Open reading frame (ORF 1ab gene) of SARS-CoV2 encodes and replicates as Orf1ab polyprotein (PP1ab). Mpro was found to cleave products of PP1ab, which are essential for multiplication and transcription process of the SARS-CoV2¹¹. In addition to globular cluster of five helices of Mpro molecule comprises as three domains, domain I and II and domain III. It is catalytic process with dimerization of protein (DOP) is required for regulation process in Glu166 residue and a key amino acid involved with the dimerization of Mpro¹³.

At present Mpro protein is mostly using for computer-based drug designing approach for the treatment of COVID-19^{14,15}. According to exist databases and natural agents against emerging targets such as viral envelop protein (EVP), spike proteins (VSPs), 2'-O-ribose methyl transferase, nucleocapsid protein (NCP), 3CL hydrolase and protease is rapidly emerging as an essential target for the development of new vaccines and potential drugs¹⁶⁻¹⁸.

Conventional drugs like Remdesivir, hydroxychloroquine, and chloroquine have been tried and found curative effect in various pre-clinical and clinical drug response¹⁹. Conventional drugs are remaining an inevitable issue, synthetic chemicals used in allopathic drugs causing serious unpleasant effects due to the fundamental side effects (FSEs). The traditional system of medicine (herbal medicine) for their primary health care (PHC) level are more useful and sizeable population has switched over to it. High-throughput technology of *in-silico* based screening approach of the important compounds against molecular targets gained much attention recently. The special challenges of antiviral drug discovery (AVDD) is possible through *in silico* screening tools²⁰.

In this process, selected compounds in libraries are screened through the various aspects of virtual screening methods such as docking and ligand-based similar searches (DLBSS), computer-aided prediction of properties (CAPPs) limiting to the small set of new candidates for their biologic testing^{21,22}. This rational approach makes the drug discovery process highly efficient, goal-oriented, and cost-effective. Extracted compounds of these selectively important species of herbal plants Turmeric (*Curcuma longa L.*) was estimated for its inhibition properties against the SARS-CoV-2. The potentiality of protease enzymes in *in Silico* approach find out the best-targeted compound in the World for first time. In this study, we performed molecular docking, interactions and ADME properties of herbal plants Turmeric (*Curcuma longa L.*) and extracted compounds against protease enzymes of SARS-CoV-2.

MATERIAL AND METHODOLOGY

Protein preparation

The 3D crystal structure of the main protease (PDB entry code: 6lu7) of SARS-CoV-2 was received from the protein databank (<http://www.rcsb.org>). Ligand and water molecules were removed from the protein molecule before the docking. The preparation of the PDB file was done using Discovery Studio 2016²³.

Ligand Preparation

We searched and found the presence of 235 phytochemicals in *Curcuma Longa L.* (Turmeric). All chemical structures of these phytochemicals downloaded from various database Pubchem, and Chempidder in SDF format.

Generation of receptor grid

Protease was subjected to the Transient Pockets in Proteins (TRAP) web server for the analysis of active sites prediction. There were 4 binding sites were generated, and the top one was selected for further analysis. The receptor grid was generated using module of maestro 12.0.

Molecular Docking

To determine the bonding affinity and other type of interactions between the compounds and the target main protease, molecular docking was done. Autodock 1.5.4 tools was used to performed docking purpose. MGL Tools package was employing default settings, a grid box (x -26.283, y 12.599, z 58.965 at 1 Angstrom spacing), the bioactive conformations were simulated employing Autodock Vina^{24,25}. For auto dock Vina study, an extended PDB format, termed PDBQT, is used for coordinate files, which includes atomic partial charges and atom types. The PyMOL used for visualization of the protein-ligand complex²⁶. The results were further observed and analyzed in Discovery studio 2016 and PyMOL^{23-25,27-29}.

ADME Properties

The web browser that displays the main submission page of the Swiss ADME accessed the SIB website <http://www.swissadme.ch>. This method is freely available and used for filtering *in silico* ADME approach³⁰. This newly developed technique has been widely accepted and used for the important screen compounds. That are expected to be reproduced within more for product design programs

(PDPs). We have tested both of the parameters such as the number of rigid bonds and number of rotatable No. bonds (> 10) that suggest good oral bioavailability and interestingly it good for the intestinal absorption of the compound³¹. The Swiss ADME also has computational filters that included in the Ghose, Egan, Veber, and Muegee developed by the leading pharmaceutical companies and cheminformaticians to evaluate the drug-likeness of these smaller molecules^{29,32,33}. Presently, Drug metabolism via CYP isoenzymes are in the important determinant of drug interactions lead to drug toxicities and reduced pharmacological effect. The models return “Yes” or “No” if the molecule under investigation has higher probability to be substrate or non-substrate of P-GP or inhibitor or non-inhibitor of a given CYP. Pertinent to P-GP and CYP enzyme kinetics is the human gastrointestinal absorption (HIA) and blood-brain barrier penetration (BBBP). In addition to the two topological methods to predict water solubility are included in Swiss ADME. He Swiss ADME is the third predictor for solubility and was developed by SILICOS.

RESULTS AND DISCUSSION

Molecular Docking

Here we reported that 235 compounds docked systematically, (Table No.1) show the binding energy (Kcal/mol) of natural compounds (BENCs) represents as *Curcuma longa L.* towards the main protease enzyme. Compare to standard inhibitor chloroquine (-6.0 Kcal/mol) we have found 36 compounds best binding energy shown in Table No.2.

Protein-ligand Interaction

In interaction of energies that is the 1st level concern the hydrogen bonds. Those of the 2nd level concerning with the interactions between p systems and cation-p interactions. We observed clearly, that the interactions of the 3rd level are hydrophobic interactions and non-specific are in Vander Waals interactions between (Aliphatic or Aromatic) carbon atoms. These interactions are general spherical with a radius of 4 Å and cover the most of the ligands. The newly displacement of ligands in the binding site of protease enzyme in the first level of interactions. In

selected complex explains that we have a good interaction between the sixteen molecules and the studied protein shown in Figure No.1-8 and Table No.3.

ADME Properties

The structural features of sixteen molecules were entered in Swiss ADME website using the Chem Axon's Marvin JS structure drawing tool.

Physicochemical Properties

The drug-likeness graph is presented as a hexagon (Figure No.17,18) with each of the vertices representing a parameter that define a drug properties. The pink area within the hexagon represents the optimal range for each property. Selected sixteen compounds show molecular weight (MW) between 150-500g/mol. All the compounds except Hopenone I show good TPSA value (20-130 Å). In Table No.4 all sixteen compounds show physicochemical properties.

Lipophilicity Properties

Lipophilicity evaluated as consensus Log P indicated all sixteen compounds (except 4''-(4'''-hydroxyphenyl-3-methoxy)-2''-oxo-3''-butenyl-3-(4'-hydroxyphenyl)-propenoate and Hopenone I) show good XLogP3 value (-0.7- +5.0) in Table No.5.

Water solubility properties

All predicted values are the decimal logarithm of the molar solubility in water (logS). Water solubility of the molecules ranged from soluble [Epiprocurcumenol, Isoprocurcumenol, Zedoaronediol, Procurcumenol, and Gitoxigenin] to Moderately [Curcumin I, 1-(4-hydroxy-3-methoxyphenyl)-7-(3, 4-dihydroxyphenyl)-1, 6-heptadiene-3, 5-dione, 1, 5-dihydroxy-1-(4-hydroxy-3-methoxyphenyl)-7-(4-hydroxyphenyl)-4,6-heptadiene-3-one, Cyclocurcumin, 1-(4-hydroxy-3-methoxyphenyl)-5-(4-hydroxyphenyl)-1,4-pentadiene-3-one, 1,5-bis(4-hydroxy-3-methoxyphenyl)-penta-(1*E*, 4*E*)-1, 4-dien-3-one, curcumin L] using the ESOL (not higher than 6) and other criteria (Table No.6).

Pharmacokinetics properties

P-glycoprotein and CYP enzyme activity prediction

Drug metabolism via CYP isoenzymes is an important determinant of drug interactions which

could lead to drug toxicities and reduced pharmacological effect. The models return "YES" or "NO" if the molecule under investigation has higher probability to be substrate or non-substrate of P-gp or inhibitor or non-inhibitor of a given CYP. All the molecules returned "No" for P-gp substrate except [4''-(4'''-hydroxyphenyl-3-methoxy)-2''-oxo-3''-butenyl-3-(4'-hydroxyphenyl)-propenoate and Gitoxigenin] "No" for CYP2D6 and CYP2C19 (Table No.7). While many compounds are deactivated by CYP3A4, there are also some compounds which are activated by the enzyme. Now, a biological experiment will be required to determine if compounds is activated or deactivated by CYP3A4.

HIA and BBB Prediction

Swiss ADME BOILED egg (Figure No.19) allows for evaluation of HIA as a function of the position of the seventeen molecules in the WLOGP-Versus-TPSA referential. Molecule 1(Control), Molecule Number 2, 3, 5, 6, 9, 11, 14, 15 and 16 are predicted as absorbed by gastro intestines (White Region) but are not brain penetrant (Yolk) (Figure No.19). All the molecules evaluated are PGP⁻ except molecule 9 (4''-(4'''-hydroxyphenyl-3-methoxy)-2''-oxo-3''-butenyl-3-(4'-hydroxyphenyl)-propenoate) and molecule 16 (Gitoxigenin) are not subject to active efflux (Red dot) (Figure No.19).

Drug likeness properties of sixteen compounds using Swiss ADME

Human passive intestinal absorption (HIA) of selected compounds governs for efflux mechanisms and active transport through Egan computation model therefore robust in predicting absorption of drugs. Exclusion of redundant descriptiontors allowed all the compounds [Except Tetrahydroxycurcumin and Hopenone I] is to obey the Egan rules (Table No.8). All the compounds have a good bioavailability score [F>10%] (Table No.8).

Medicinal chemistry evaluation of the sixteen compounds

PAINS is screening computer model that identify compounds that appear as hits in many biochemical high throughput screens. Swiss ADME evaluation did not post any PAINS alert of the compounds [Except 1-(4-hydroxy-3-methoxyphenyl)-7-(3,

4dihydroxyphenyl)-1,6-heptadiene-3,5-Dione]
shown in Table No.9.

Table No.1: All compounds docking results

N ⁰ Compounds	Phytochemicals	Binding Energy (Kcal/mol)	N ⁰ Compounds	Phytochemicals	Binding Energy (Kcal/mol)
1	Curcumin (curcumin I)	-6.5	2	Demethoxycurcumin (curcumin II)	-6.0
3	1-(4-hydroxy-3-methoxyphenyl)-7-(3, 4-dihydroxyphenyl)-1, 6-heptadiene-3, 5-dione	-6.3	4	1-(4-hydroxyphenyl)-7-(3, 4-dihydroxyphenyl)-1, 6-heptadiene-3, 5-dione	-6.7
5	Bisdemethoxycurcumin (curcumin III)	-6.0	6	Tetrahydroxycurcumin	-6.5
7	5-hydroxyl-1-(4-hydroxy-3-methoxyphenyl)-7-(4-hydroxyphenyl)-4, 6-heptadiene-3-one	-5.7	8	5-hydroxyl-1,7-bis(4-hydroxy-3-methoxyphenyl)-4, 6-heptadiene-3-on	-5.8
9	1, 7-bis(4-hydroxyphenyl)-1-heptene-3, 5-dione	-5.6	10	5-hydroxyl-7-(4-hydroxy-3-methoxyphenyl)-1-(4-hydroxyphenyl)-4, 6-heptadiene-3-one	-5.0
11	3-hydroxy-1, 7-bis-(4-hydroxyphenyl)-6-heptene-1, 5-dione	-5.3	12	1, 5-dihydroxy-1-(4-hydroxy-3-methoxyphenyl)-7-(4-hydroxyphenyl)-4, 6-heptadiene-3-one	-6.6
13	1, 5-dihydroxy-1-(4-hydroxyphenyl)-7-(4-hydroxy-3-methoxyphenyl)-4, 6-heptadiene-3-one	4.5	14	1, 5-dihydroxy-1, 7-bis(4-hydroxy-3-methoxyphenyl)-4, 6-heptadiene-3-one	-4.9
15	1, 5-dihydroxy-1, 7-bis(4-hydroxyphenyl)-4, 6-heptadiene-3-one	-6.0	16	1, 5-epoxy-3-carbonyl-1, 7-bis(4-hydroxyphenyl)-4, 6-heptadiene	-5.6
17	Cyclocurcumin	-8.2	18	1, 7-bis(4-hydroxy-3-methoxyphenyl)-1, 4, 6-heptatrien-3-one	-6.3
19	1, 7-bis-(4-hydroxyphenyl)-1, 4, 6-heptatrien-3-one	-6.5	20	1, 5-bis(4-hydroxyphenyl)-penta-(1E,4E)-1, 4-dien-3-one	-7.5
21	1-(4-hydroxy-3-methoxyphenyl)-5-(4-hydroxyphenyl)-1, 4-pentadiene-3-one	-6.2	22	1, 5-bis(4-hydroxy-3-methoxyphenyl)-penta-(1E,4E)-1, 4-dien-3-one	-6.1
23	4''-(4'''-hydroxyphenyl)-2''-oxo-3''-butenyl-3-(4'	6.0	24	4''-(4'''-hydroxyphenyl)-3-methoxy)-2''-oxo-3''-butenyl-	-8.6

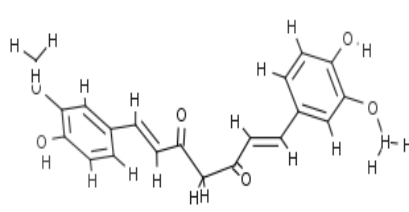
	hydroxyphenyl-3'-methoxy)-propenoate			3-(4'-hydroxyphenyl)-propenoate	
25	Calebin-A	-5.5	26	(<i>E</i>)-4-(4-hydroxy-3-methoxyphenyl)but-3-en-2-one	-5.1
27	(<i>E</i>)-ferulic acid	-5.7	28	(<i>Z</i>)-ferulic acid	-5.5
29	Vanillic acid*	-5.4	30	Vanillin	-5.7
31	<i>P</i> -cymene*	-4.9	32	<i>M</i> -cymene *	-5.1
33	α -terpinene*	-5.0	34	Γ -terpinene*	-5.5
35	β -phellandrene*	-5.4	36	<i>P</i> -mentha-1,4(8)-diene*	-5.2
37	Terpinen-4-ol*	-5.1	38	4-terpinol*	-4.7
39	Limonene*	-5.1	40	Terpinolene*	-4.9
41	Thymol*	-5.2	42	Phellandrol*	-6.0
43	Carvacrol*	-5.3	44	(<i>E</i>)-carveol*	-4.9
45	Γ -terpineol*	-3.0	46	Menthol	-5.3
47	1, 3, 8-paramenthatriene	-5.0	48	<i>P</i> -methylacetophenone	-5.0
49	Piperitone	-4.9	50	<i>O</i> -cymene*	-5.2
51	Carvone*	-4.9	52	<i>P</i> -menth-8-en-2-one*	-4.9
53	<i>A</i> -thujene*	-4.5	54	<i>A</i> -terpineol*	4.7
55	<i>P</i> -cymen-8-ol*	-5.3	56	<i>P</i> -meth-8-en-2-one*	-4.7
57	Piperitone epoxide*	-5.0	58	Sylvestrene*	-5.2
59	Menthofuran*	-5.8	60	<i>B</i> , β -dimethylstyrene	-4.0
61	Camphor	-5.3	62	Teresantalol	-5.1
63	Benzene, 1-methyl-4-(1-methylpropyl)	-5.2	64	2-norpinanone*	-5.0
65	Borneol*	-6.0	66	Bornyl acetate*	-5.7
67	(<i>E</i>)-chrysanthenyl acetate*	-5.5	68	(<i>Z</i>)-cinerone*	-4.8
69	(<i>Z</i>)-sabinol*	-4.9	70	2-(2, 5-dihydroxy-4-methylcyclohex-3-enyl) propanoic acid	-4.0
71	Camphene*	-5.0	72	3-carene*	-5.0
73	2-carene*	-4.8	74	Ascaridole*	-5.1
75	α -pinene*	-3.0	76	β -pinene*	-4.0
77	Cineole*	-5.1	78	<i>Cis</i> -ocimene*	-4.8
79	Citronellal*	-4.1	80	Geranial*	-4.5
81	Neral*	-4.7	82	Myrcene*	-4.4
83	<i>R</i> -citronellene*	-2.2	84	Citronellyl pentanoate*	-4.9
85	Nerol*	-4.9	86	Geraniol	-4.4
87	Iso-artemisia ketone*	-4.3	88	<i>Trans</i> -ocimene*	-4.5
89	Linalool*	-4.4	90	Neryl acetate	-4.8
91	Geranic acid	-5.1	92	Geranyl acetate	-4.4
93	3-bornanone	-	94	4, 8-dimethyl-3,7-nonadien-2-ol	-4.8

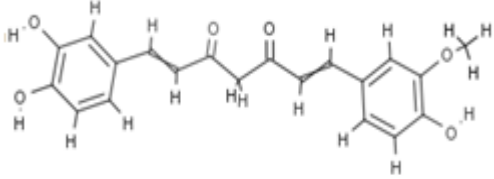
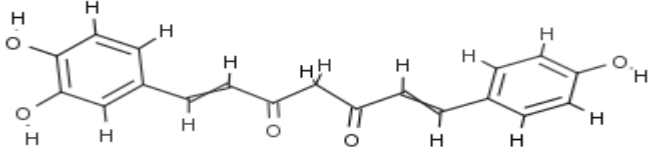
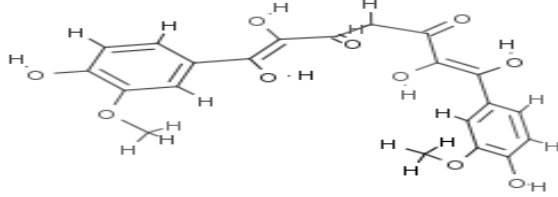
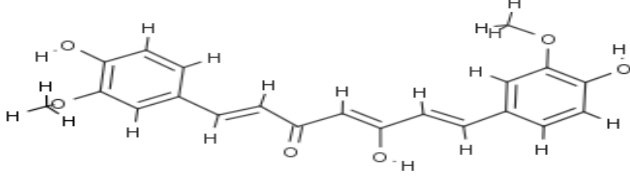
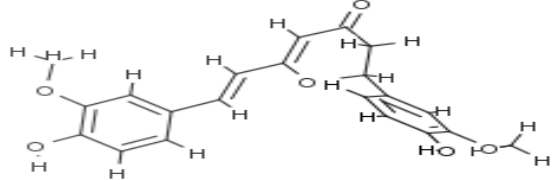
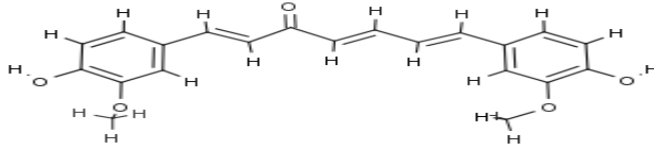
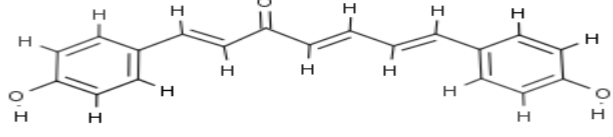
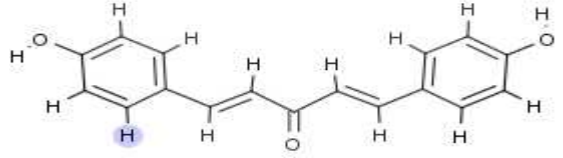
95	3, 4, 5, 6-tetramethyl-2, 5-octadiene	-4.9	96	3,7-dimethyl-6-nonenal	-4.4
97	2, 6-dimethyl-2, 6-octadiene-1, 8-diol	-5.0	98	4, 5-dimethyl-2, 6-octadiene	-4.3
99	<i>Ar</i> -turmerone*	-5.7	100	<i>A</i> -turmerone*	.50
101	β -turmerone*	-	102	2-methyl-6-(4-hydroxyphenyl)-2-hepten-4-one	-5.7
103	2-methyl-6-(4-hydroxy-3-methylphenyl)-2-hepten-4-one	-6.1	104	2-methoxy-5-hydroxybisabola-3,10-diene-9-one	5.0
105	2-methyl-6-(4-formylphenyl)-2-hepten-4-one	5.0	106	5-hydroxyl- <i>ar</i> -turmerone	-5.9
107	4-methylene-5-hydroxybisabola-2,10-diene-9-one	-3.0	108	<i>ar</i> -curcumene*	-5.0
109	<i>ar</i> -turmerol*	-4.9	110	bisabola-3, 10-diene-2-one	-5.1
111	Bisabolone	-5.4	112	4, 5-dihydroxybisabola-2,10-diene	5.5
113	4-hydroxybisabola-2, 10-diene-9-one	-5.6	114	4-methoxy-5-hydroxybisabola-2, 10-diene-9-one	-5.4
115	Bisacurone	-5.5	116	bisacurone A	-5.8
117	bisacurone B	-5.9	118	bisacurone C	-5.9
119	bisabolone-9-one	-4.2	120	Bisacumol	-5.6
121	turmeronol A	-5.9	122	turmeronol B	-5.5
123	α -oxobisabolene*	-6.0	124	α -zingiberene	-4.5
125	xanthorrhizol*	-5.6	126	Zingerone	-5.4
127	Dehydrozingerone	-5.4	128	(<i>Z</i>)- α -atlantone*	-5.9
129	(<i>E</i>)- α -atlantone*	5.0	130	β -bisabolene*	-4.6
131	(6 <i>S</i> , 7 <i>R</i>)-bisabolene*	-5.5	132	γ -bisabolene*	-3.5
133	γ -curcumene*	-4.9	134	β -curcumene*	-5.1
135	α -curcumene*	-5.2	136	β -sesquiphellandrene*	-5.0
137	(<i>Z</i>)- α -atlantone*	-3.0	138	(<i>E</i>)- γ -atlantone	-3.6
139	(6 <i>S</i>)-2-methyl-6-[(1 <i>R</i> ,5 <i>S</i>)-(4-methene-5-hydroxyl-2-cyclohexen)-2-hepten-4-one	-5.8	140	curcuphenol*	-5.6
141	Curlone	-4.9	142	curculonone C	-5.5
143	curculonone D	-5.8	144	curculonone B	-5.1
145	curculonone A	-5.4	146	2, 5-dihydroxybisabola-3, 10-diene	-4.5
147	(6 <i>R</i>)-[(1 <i>R</i>)-1, 5-dimethylhex-4-enyl]-3-methylcyclohex-2-en-1-one	-5.4	148	β -atlantone	-5.7
149	2, 8-epoxy-5-hydroxybisabola-3, 10-diene-9-one	-4.2	150	α -bisabolol	-4.3

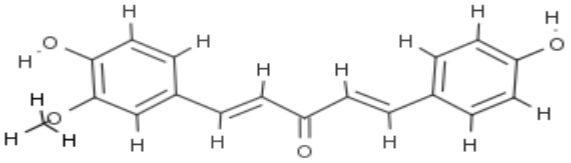
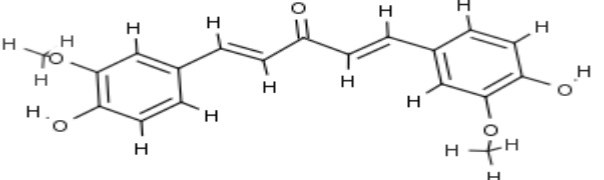
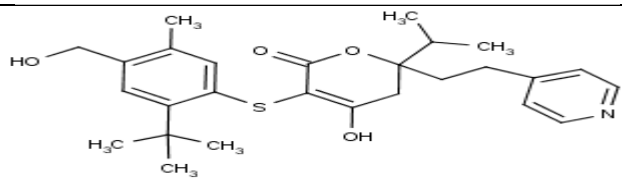
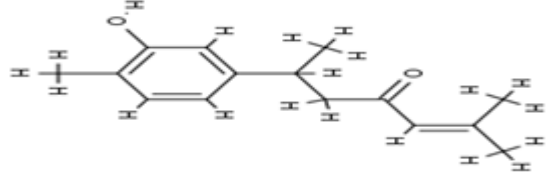
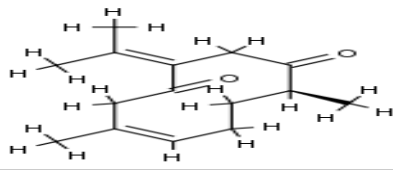
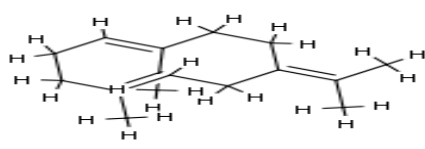
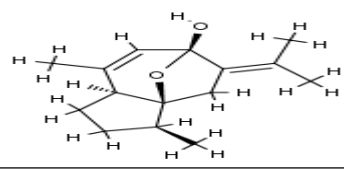
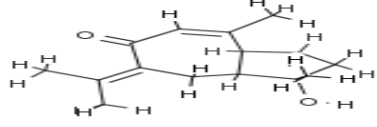
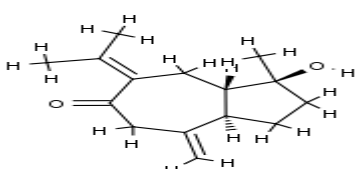
151	dihydro-ar-turmerone	-5.0	152	dehydrocurcumene	-5.7
153	(4 <i>S</i> , 5 <i>S</i>)-germacrone-4, 5-epoxide	-6	154	Dehydrocurdione	-6.2
155	germacrene D*	-6	156	Germacrone	-6
157	germacrone-13-al	-5.7	158	β -germacene*	-6.4
159	1, 10-dehydro-10-deoxy-9-oxozedoarondiol	5.0	160	Curcumenol	-6.5
161	Epiprocurcumenol	-6.3	162	Isoprocurcumenol	-6.3
163	Zedoaronediol	-6.3	164	Procurcumadiol	-6.0
165	Procurcumenol	-6.5	166	naphthalene, 1, 2, 3, 4, 4a, 5, 6, 8a-octahydro-4a, 8-dimethyl-2-(1-methylethylidene)	-5.9
167	α -selinene	-5.3	168	juniper camphor	-6.5
169	corymbolone*	-6.1	170	α -santalol	-3.0
171	α -santalene	-4.5	172	β -santalene	-5.1
173	(<i>E</i>)-caryophyllene*	-5.9	174	caryophyllene oxide	-6.3
175	β -elemene*	5.8	176	γ -elemene	-4.7
177	Acoradiene	-6.1	178	Aristolene	-6.2
179	(<i>Z</i>)- α -bergamotene*	-5.6	180	Curcumenone	-5.5
181	di-epi-cedrene	-6	182	Himachalene	-6.0
183	(<i>E</i>)-sesquisabinene hydrate*	-5.5	184	Bicycle [7.2.0] undecane, 10, 10-dimethyl-2, 6-bis(methylene)	-6.3
185	γ -gurjunen epoxide	-5.0	186	1-epi-cubenol	-5.9
187	cubebene*	-6.3	188	7-epi-sesquithujene*	-5.1
189	caryophyllene*	-6.0	190	6- α -hydroxycurcumanolide A	-6.0
191	curcumanolide A	-6.1	192	curcumanolide B	-6.0
193	curcumin L	-6.5	194	α -humulene*	-5.0
195	12-oxabicyclo[9.1.0]dodeca-3, 7-diene, 1, 5, 5, 8-tetramethyl-	-5.7	196	Adoxal	-4.8
197	2, 6, 10-dodecatrien-1-ol, 3, 7, 11-trimethyl-	-5.4	198	(<i>E,E</i>)- α -farnesene*	-4.0
199	5, 9-undecadien-2-one, 6, 10-dimethyl-, (<i>Z</i>)-	-5.1	200	hxadecane-1, 2-diol*	-5.0
201	Nerolidal	-5.7	202	(<i>Z</i>)- β -farnesene*	-4.1
203	nerolidyl propionate	-4.5	204	phytol*	-4.3
205	(<i>E,E,E</i>)-3, 7, 11, 15-tetramethylhexadeca-1, 3, 6, 10, 14-pentaene	-5.2	206	2, 6, 11, 15-tetramethylhexadeca-2, 6, 8, 10, 14-pentaene	-5.3
207	1, 6, 10, 14-hexadecatetraen-3-ol, 3, 7, 11, 15-tetramethyl-, (<i>E, E</i>)-	-5.0	208	hopenone I	-8.2
209	hop-17(21)-en-3 β -ol	-3.0	210	hop-17(21)-en-3 β -yl acetate	-4.0

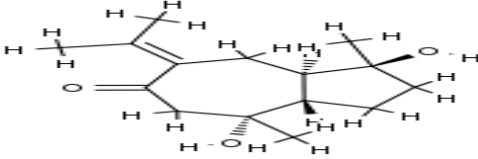
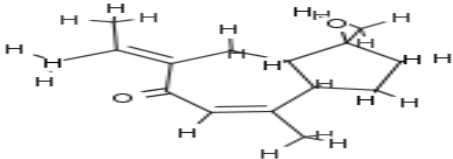
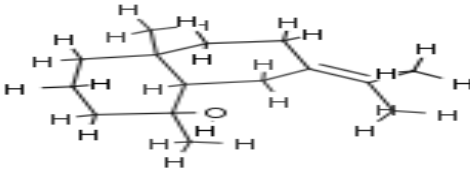
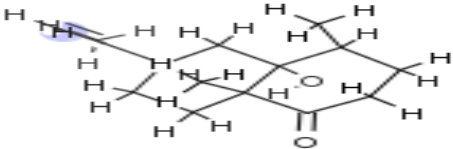
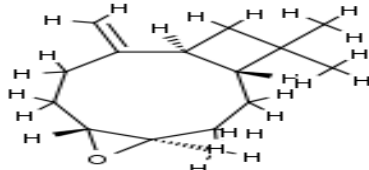
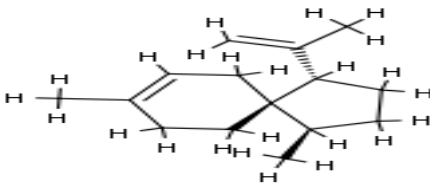
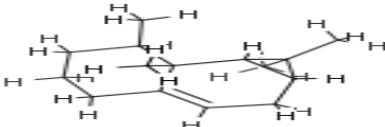
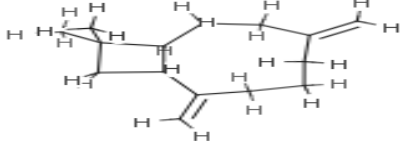
211	β -sitosterol	-7.5	212	Stigmasterol	-7.1
213	Gitoxigenin	-7.2	214	20-oxopregn-16-en-12-yl acetate	-7.4
215	linoleic acid*	-4.8	216	8,11-Octadecadienoic acid, methyl ester *	-4.4
217	palmitic acid (n-hexadecanoic acid)*	-4.0	218	oleic acid*	-4.3
219	stearic acid*	-5.1	220	curcuma-J	-5.8
221	2-(2'-methyl-1'-propenyl)-4, 6-dimethyl-7-hydroxyquinoline	-5.9	222	2, 3, 5-trimethylfuran	-4.0
223	(1, 2, 3-trimethyl-cyclopent-2-enyl)-methanol	-5.0	224	dicumyl peroxide	-6.4
225	1-(3-cyclopentylpropyl)-2,4-dimethyl-benzene,	-5.4	226	1, 4-dimethyl-2-(2-methylpropyl)-benzene	-5.4
227	2, 2'-oxybis[octahydro-7, 8, 8-trimethyl-4, 7-methanobenzofuran	-9.9	228	cyclohexylformate	-4.4
229	Methyleugenol	-4.5	230	3, 3, 5-trimethyl-cyclohexanol acetate	-5.1
231	2, 4-dimethyl-8-oxabicyclo[3.2.1]oct-6-en-3-one	-5.2	232	2, 6-dimethyl-6-(4-methyl-3-pentenyl)-2-cyclohexene-1-carboxaldehyde	-5.4
233	bicyclo[3.3.1]nonan-9-one, 2,4-dimethyl-3-nitro- (exo)-	-5.7	234	2, 2, 4-trimethyl-3-(3, 8, 12, 16-tetramethyl-heptadeca-3, 7, 11, 15-tetraenyl)-cyclohexanol	-5.4
235	pyrazolo[1, 5-a]pyridine, 3, 3a, 4, 7-tetrahydro-3,3-dimethyl-, (3aS)	-5.3	---	---	---

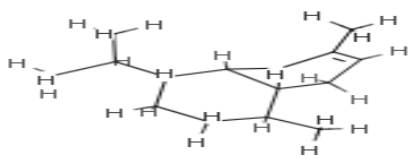
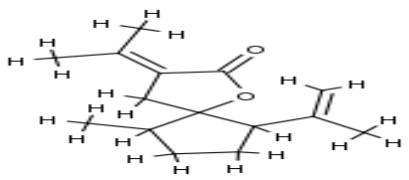
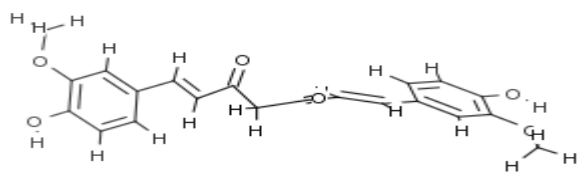
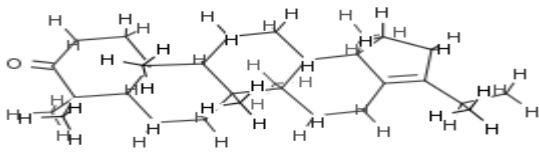
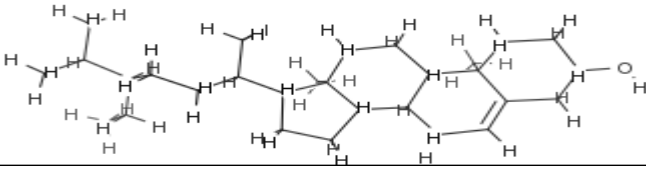
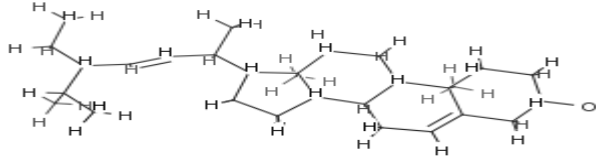
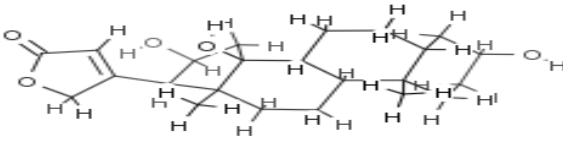
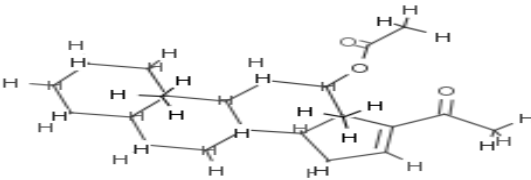
Table No.2: Top 36 compounds docking results

N ^o Compounds	Compounds Name	Structure	Binding Affinity (Kcal/mol)
1	curcumin (curcumin I)		-6.5

3	1-(4-hydroxy-3-methoxyphenyl)-7-(3, 4-dihydroxyphenyl)-1, 6-heptadiene-3, 5-dione		-6.3
4	1-(4-hydroxyphenyl)-7-(3, 4-dihydroxyphenyl)-1, 6-heptadiene-3, 5-dione		-6.7
6	Tetrahydroxycurcumin		-6.5
12	1, 5-dihydroxy-1-(4-hydroxy-3-methoxyphenyl)-7-(4-hydroxyphenyl)-4, 6-heptadiene-3-one		-6.6
17	Cyclocurcumin		-8.2
18	1, 7-bis(4-hydroxy-3-methoxyphenyl)-1, 4, 6-heptatrien-3-one		-6.3
19	1, 7-bis-(4-hydroxyphenyl)-1, 4, 6-heptatrien-3-one		-6.5
20	1, 5-bis(4-hydroxyphenyl)-penta-(1E,4E)-1, 4-dien-3-one		-7.5

21	1-(4-hydroxy-3-methoxyphenyl)-5-(4-hydroxyphenyl)-1, 4-pentadiene-3-one		-6.2
22	1, 5-bis (4-hydroxy-3-methoxyphenyl)-penta-(1E,4E)-1, 4-dien-3-one		-6.1
24	4''-(4'''-hydroxyphenyl-3-methoxy)-2''-oxo-3''-butenyl-3-(4'-hydroxyphenyl)-propenoate		-8.6
103	2-methyl-6-(4-hydroxy-3-methylphenyl)-2-hepten-4-one		-6.1
154	Dehydrocurdione		-6.2
158	β -germacene*		-6.4
160	Curcumeno		-6.5
161	Epiprocurcumenol		-6.3
162	Isoprocurcumenol		-6.3

163	Zedoaronediol		-6.3
165	Procurcumenol		-6.5
168	juniper camphor		-6.5
169	corymbolone*		-6.1
174	caryophyllene oxide		-6.3
177	Acoradiene		-6.1
178	Aristolene		-6.2
184	Bicyclo [7.2.0] undecane, 10, 10-dimethyl-2, 6-bis (methylene)		-6.3

187	cubebene*		-6.3
191	curcumanolide A		-6.1
193	curcumin L		-6.5
208	hopenone I		-8.2
211	β -sitosterol		-7.5
212	Stigmasterol		-7.1
213	Gitoxigenin		-7.2
214	20-oxopregn-16-en-12-yl acetate		-7.4

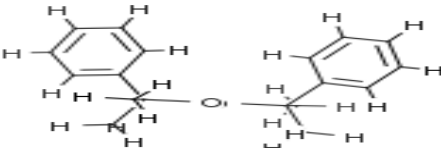
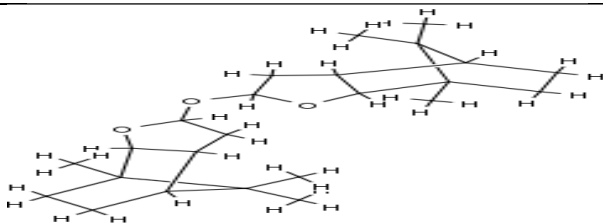
224	dicumyl peroxide		-6.4
227	2, 2'-oxybis[octahydro-7, 8, 8-trimethyl-4, 7-methanobenzofuran		-9.9

Table No.3: Hydrogen bond interaction between the sixteen natural compounds and Coronavirus (2019-nCoV) main protease

Molecule No.	Compounds Name and Pubchem id	Residue formed Hydrogen bond interaction with studied compounds
1	Curcumin (curcumin I) Pubchem Id- 969516	Arg A:105, Ser A:158
2	1-(4-hydroxy-3-methoxyphenyl)-7-(3, 4-dihydroxyphenyl)-1, 6-heptadiene-3, 5-dione Pubchem Id-390474	Leu A: 287, Arg A:131, Asn A: 238, Asp A: 197
3	Tetrahydrocurcumin Pubchem Id-129762283	Lys A:137, Asp A: 289, Leu A:287, Tyr A:237, Glu A:288
4	1, 5-dihydroxy-1-(4-hydroxy-3-methoxyphenyl)-7-(4-hydroxyphenyl)-4, 6-heptadiene-3-one Pubchem Id-5281767	Lys A:137, Lys A:5
5	Cyclocurcumin Pubchem Id-69879809	Gly A:71
6	1-(4-hydroxy-3-methoxyphenyl)-5-(4-hydroxyphenyl)-1, 4-pentadiene-3-one Pubchem Id-10469828	Ile A:152
7	1, 5-bis (4-hydroxy-3-methoxyphenyl)-penta-(1E, 4E)-1, 4-dien-3-one Pubchem Id-6474893	Lys A:137, Arg A:131
8	4''-(4'''-hydroxyphenyl-3-methoxy)-2''-oxo-3''-butenyl-3-(4'-hydroxyphenyl)-propenoate Pubchem Id-637432	Gln A:110
9	Epiprocurcumenol Pubchem Id-10263440	Arg A:279, Gly A:275
10	Isoprocurcumenol Pubchem Id-14543198	Leu A:271
11	Zedoaronediol Pubchem Id-101792719	Asn A:277, Arg A:279, Phe A:219, Asn A:221

12	Procurecumenol Pubchem Id-18961	Asn A:221, Glu A:270, Asn A:274
13	Curcumin L Pubchem Id-969516	Arg A:105, Ser A:158
14	Hopenone I Pubchem Id-21603525	Arg A:131
15	Gitoxigenin Pubchem Id-348482	Arg A:131, Leu A:287, Asp A:289
16	20-oxopregn-16-en-12-yl acetate Pubchem Id-22295917	Arg A:131

Table No.4: Physicochemical properties of the sixteen selected molecules

Molecule Number	Formula	Molecular weight	Num. heavy atoms	Num. arom. heavy atoms	Fraction Csp3	Num. rotatable bonds	Num. H-bond acceptors	Num. H-bond donors	Molar Refractivity	TPSA
1	C21H20O6	368.38g/mol	27	12	0.14	8	6	2	102.80	93.06Å ²
2	C15H24O3	252.35g/mol	18	0	0.8	0	3	2	72.12	57.53Å ²
3	C15H24O3	252.35g/mol	18	0	0.8	0	3	2	72.12	57.53Å ²
4	C21H20O6	368.38g/mol	27	12	0.10	7	6	3	103.70	96.22Å ²
5	C21H20O6	368.38g/mol	27	12	0.19	5	6	2	100.78	85.22Å ²
6	C18H16O4	296.32g/mol	22	12	0.06	5	4	2	86.50	66.76Å ²
7	C19H18O5	326.34g/mol	24	12	0.11	6	5	2	92.99	75.99Å ²
8	C27H35NO4S	469.64g/mol	33	12	0.48	8	5	2	134.38	104.95Å ²
9	C15H22O2	234.33g/mol	17	0	0.67	0	2	1	70.44	37.30 Å ²
10	C15H22O2	234.33g/mol	17	0	0.67	0	2	1	70.44	37.30 Å ²
11	C15H24O3	252.35g/mol	18	0	0.80	0	3	2	72.12	57.53 Å ²
12	C15H22O2	234.33g/mol	17	0	0.67	0	2	1	70.44	37.30Å ²
13	C21H20O6	368.38g/mol	27	12	0.14	8	6	2	102.80	93.06Å ²
14	C30H48O	424.70g/mol	31	0	0.90	1	1	0	134.18	17.07Å ²
15	C23H34O5	390.51g/mol	28	0	0.87	1	5	3	105.92	86.99Å ²
16	C23H34O3	358.51g/mol	26	0	0.83	3	3	0	104.71	43.37Å ²

Table No.5: Lipophilicity properties of sixteen selected molecules

Molecule No	Log P _{o/w} (iLOGP)	Log P _{o/w} (XLOGP3)	Log P _{o/w} (WLOGP)	Log P _{o/w} (MLOGP)	Log P _{o/w} (SILICOS-IT)	Consensus Log P _{o/w}
1	3.27	3.20	3.15	1.47	4.04	3.03
2	2.63	2.87	2.85	1.25	3.48	2.62
3	1.46	2.89	2.91	-1.66	1.06	1.33
4	3.21	3.98	3.63	1.47	3.55	3.17
5	3.12	3.00	3.31	1.16	3.50	2.82
6	2.69	3.46	3.18	2.24	3.60	3.08
7	3.10	3.35	3.19	1.91	3.67	3.05
8	3.87	5.93	5.86	3.31	6.54	5.10
9	2.61	3.34	3.02	2.54	3.02	2.71

10	2.60	2.26	3.02	2.54	3.31	2.75
11	2.45	1.60	2.21	1.75	2.54	2.11
12	2.56	2.34	3.02	2.54	3.02	2.70
13	3.27	3.20	3.15	1.47	4.04	3.03
14	4.64	8.25	8.38	6.82	7.78	7.17
15	2.84	1.60	2.58	2.73	2.55	2.46
16	3.28	5.69	5.09	4.31	4.37	4.55

Table No.6: Water Solubility properties of sixteen selected molecules

Molecule No.	Log S (ESOL)	Solubility	Class	Log S (Ali)	Solubility	Class	Log S (SILI COS-IT)	Solubility	Class
1	-3.94	4.22e-02mg/ml; 1.15e-04mol/l	Soluble	-4.83	5.50e-03mg/ml; 1.49e-05 mol/l	Moderately soluble	-4.45	1.31e-02mg/ml; 3.56e-05mol/l	Moderately soluble
2	-3.72	6.68e-02mg/ml; 1.89e-04mol/l	Soluble	-4.71	6.84e-03mg/ml; 1.93e-05mol/l	Moderately soluble	-3.76	6.20e-02mg/ml; 1.75e-04mol/l	Soluble
3	-4.10	3.44e-02mg/ml; 7.95e-05mol/l	Moderately soluble	-6.20	2.70e-04mg/ml; 6.26e-07mol/l	Poorly soluble	-2.10	3.47e+00mg/ml; 8.04e-03mol/l	Soluble
4	-4.50	1.17e-02mg/ml; 3.18e-05mol/l	Moderately soluble	-5.70	7.32e-04mg/ml; 1.99e-06mol/l	Moderately soluble	-3.61	9.02e-02mg/ml; 2.45e-04mol/l	Soluble
5	-4.01	3.58e-02mg/ml; 9.71e-05mol/l	Moderately soluble	-4.45	1.30e-02mg/ml ; 3.52e-05mol/l	Moderately soluble	-4.59	9.36e-03mg/ml; 2.54e-05mol/l	Moderately soluble
6	-3.93	3.48e-02mg/ml; 1.17e-04mol/l	Soluble	-4.54	8.48e-03 mg/ml; 2.86e-05mol/l	Moderately soluble	-4.01	2.89e-02mg/ml; 9.75e-05mol/l	Moderately soluble
7	-3.95	3.68e-02mg/ml; 1.13e-04mol/l	Soluble	-4.62	7.77e-03mg/ml; 2.38e-05mol/l	Moderately soluble	-4.12	2.45e-02mg/ml; 7.52e-05mol/l	Moderately soluble
8	-6.23	2.77e-04mg/ml; 5.91e-07mol/l	Poorly soluble	-7.91	5.79e-06mg/ml; 1.23e-08mol/l	Poorly soluble	-7.97	5.06e-06mg/ml; 1.08e-08mol/l	Poorly soluble
9	-2.77	4.01e-01mg/ml; 1.71e-03mol/l	Soluble	-2.76	4.05e-01mg/ml; 1.73e-03mol/l	Soluble	-2.83	3.43e-01mg/ml; 1.46e-03mol/l	Soluble
10	-2.72	4.50e-01mg/ml; 1.92e-03mol/l	Soluble	-2.68	4.90e-01mg/ml; 2.09e-03mol/l	Soluble	-3.08	1.94e-01mg/ml; 8.26e-04mol/l	Soluble
11	-2.41	9.76e-01mg/ml; 3.87e-03mol/l	Soluble	-2.42	9.60e-01mg/ml; 3.80e-03mol/l	Soluble	-2.50	8.07e-01mg/ml; 3.20e-03mol/l	Soluble
12	-2.77	4.01e-01mg/ml; 1.71e-03mol/l	Soluble	-2.76	4.05e-01mg/ml; 1.73e-03mol/l	Soluble	-2.83	3.43e-01mg/ml; 1.46e-03mol/l	Soluble
13	-3.94	4.22e-02mg/ml; 1.15e-04 mol/l	Soluble	-4.83	5.50e-03mg/ml; 1.49e-05mol/l	Moderately soluble	-4.45	1.31e-02mg/ml ; 3.56e-05mol/l	Moderately soluble
14	-7.60	1.06e-05mg/ml; 2.49e-08mol/l	Poorly soluble	-8.47	1.44e-06mg/ml; 3.38e-09mol/l	Poorly soluble	-7.86	5.86e-06mg/ml; 1.38e-08mol/l	Poorly soluble
15	-3.20	2.45e-01mg/ml; 6.26e-04mol/l	Soluble	-3.04	3.58e-01mg/ml; 9.16e-04mol/l	Soluble	-2.65	8.80e-01mg/ml; 2.25e-03mol/l	Soluble
16	-5.45	1.27e-03mg/ml; 3.55e-06mol/l	Moderately soluble	-6.37	1.54e-04 mg/ml ; 4.30e-07 mol/l	Poorly soluble	-4.31	1.75e-02mg/ml; 4.88e-05mol/l	Moderately soluble

Table No.7: Pharmacokinetics properties of sixteen selected molecules

Molecule No.	GI absorption	BBB permeant	P-gp substrate	CYP1A2 inhibitor	CYP2C19 inhibitor	CYP2C9 inhibitor	CYP2D6 inhibitor	CYP3A4 inhibitor	Log K _p (skin permeation)
1	High	No	No	No	No	Yes	No	Yes	-6.28cm/s
2	High	No	No	No	No	Yes	No	Yes	-6.42cm/s
3	Low	No	No	No	No	Yes	No	Yes	-6.89cm/s
4	High	No	No	No	No	Yes	No	Yes	-5.72cm/s
5	High	No	No	No	No	Yes	No	Yes	-6.42cm/s

6	High	Yes	No	Yes	No	Yes	No	Yes	-5.65cm/s
7	High	Yes	No	Yes	No	Yes	No	Yes	-5.91cm/s
8	Low	No	Yes	No	No	No	No	Yes	-4.95cm/s
9	High	Yes	No	No	No	No	No	No	-6.07cm/s
10	High	Yes	No	No	No	No	No	No	-6.12cm/s
11	High	Yes	No	No	No	No	No	No	-6.70cm/s
12	High	Yes	No	No	No	No	No	No	-6.07cm/s
13	High	No	No	No	No	Yes	No	Yes	-6.28cm/s
14	Low	No	No	No	No	No	No	No	-3.03cm/s
15	High	No	Yes	No	No	No	No	No	-7.55cm/s
16	High	Yes	No	No	No	Yes	No	No	-4.45cm/s

Table No.8: Drug-likeness Properties of sixteen selected molecules

Molecule No	Lipinski	Ghose	Veber	Egan	Muegge	Bioavailability Score
1	Yes; 0 violation	Yes	Yes	Yes	Yes	0.55
2	Yes; 0 violation	Yes	Yes	Yes	Yes	0.55
3	Yes; 1 violation: NHorOH>5	Yes	No; 1 violation: TPSA>140	No; 1 violation: TPSA>131.6	No; 2 violations: TPSA>150, H-don>5	0.11
4	Yes; 0 violation	Yes	Yes	Yes	Yes	0.56
5	Yes; 0 violation	Yes	Yes	Yes	Yes	0.56
6	Yes; 0 violation	Yes	Yes	Yes	Yes	0.55
7	Yes; 0 violation	Yes	Yes	Yes	Yes	0.55
8	Yes; 0 violation	No; 2 violations: WLOGP>5.6, MR>130	Yes	Yes	No; 1 violation: XLOGP3>5	0.56
9	Yes; 0 violation	Yes	Yes	Yes	Yes	0.55
10	Yes; 0 violation	Yes	Yes	Yes	Yes	0.55
11	Yes; 0 violation	Yes	Yes	Yes	Yes	0.55
12	Yes; 0 violation	Yes	Yes	Yes	Yes	0.55
13	Yes; 0 violation	Yes	Yes	Yes	Yes	0.55
14	Yes; 1 violation: MLOGP>4.15	No; 3 violations: WLOGP>5.6, MR>130, #atoms>70	Yes	No; 1 violation: WLOGP>5.88	No; 2 violations: XLOGP3>5, Heteroatoms<2	0.55
15	Yes; 0 violation	Yes	Yes	Yes	Yes	0.55
16	Yes; 1 violation: MLOGP>4.15	Yes	Yes	Yes	No; 1 violation: XLOGP3>5	0.55

Table No.9: Medicinal chemistry properties of sixteen selected molecules

Molecule No	PAINS	Brenk	Lead likeness	Synthetic accessibility
1	0 alert	2 alerts: beta_keto_anhydride, michael_acceptor_1	No; 2 violations: MW>350, Rotors>7	2.97
2	1 alert: catechol_A	3 alerts: beta_keto_anhydride, catechol, michael_acceptor_1	No; 1 violation: MW>350	2.86
3	0 alert	3 alerts: acyclic=C-O, beta_keto_anhydride, michael_acceptor_1	No; 2 violations: MW>350, Rotors>7	3.45
4	0 alert	3 alerts: acyclic=C-O, michael_acceptor_1, polyene	No; 2 violations: MW>350, XLOGP3>3.5	3.42
5	0 alert	0 alert	No; 1 violation: MW>350	4.21
6	0 alert	1 alert: michael_acceptor_1	Yes	2.61
7	0 alert	1 alert: michael_acceptor_1	Yes	2.76

8	0 alert	0 alert	No; 3 violations: MW>350, Rotors>7, XLOGP3>3.5	4.90
9	0 alert	1 alert: michael_acceptor_1	No; 1 violation: MW<250	4.04
10	0 alert	2 alerts: isolated_alkene, michael_acceptor_1	No; 1 violation: MW<250	3.89
11	0 alert	1 alert: michael_acceptor_1	Yes	4.13
12	0 alert	1 alert: michael_acceptor_1	No; 1 violation: MW<250	4.04
13	0 alert	2 alerts: beta_keto_anhydride, michael_acceptor_1	No; 2 violations: MW>350, Rotors>7	2.97
14	0 alert	1 alert: isolated_alkene	No; 2 violations: MW>350, XLOGP3>3.5	6.12
15	0 alert	0 alert	No; 1 violation: MW>350	5.70
16	0 alert	0 alert	No; 2 violations: MW>350, XLOGP3>3.5	5.31

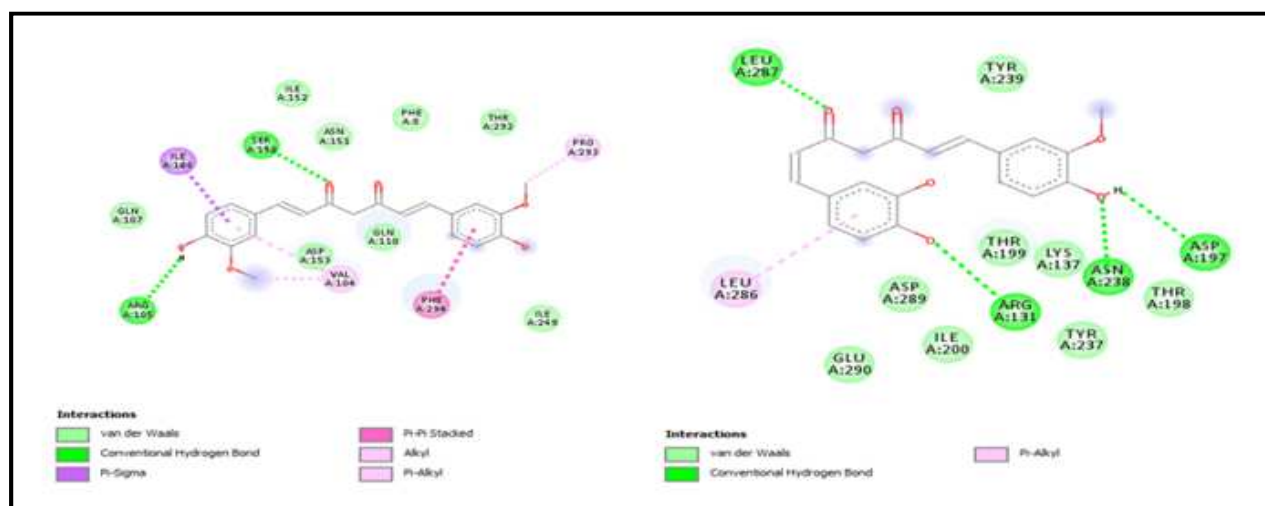


Figure No.1: 2D View of the Binding Conformation of molecule 1 and 2 at the active site of Coronavirus (2019-nCoV) main Protease. (Hydrogen bond interaction)

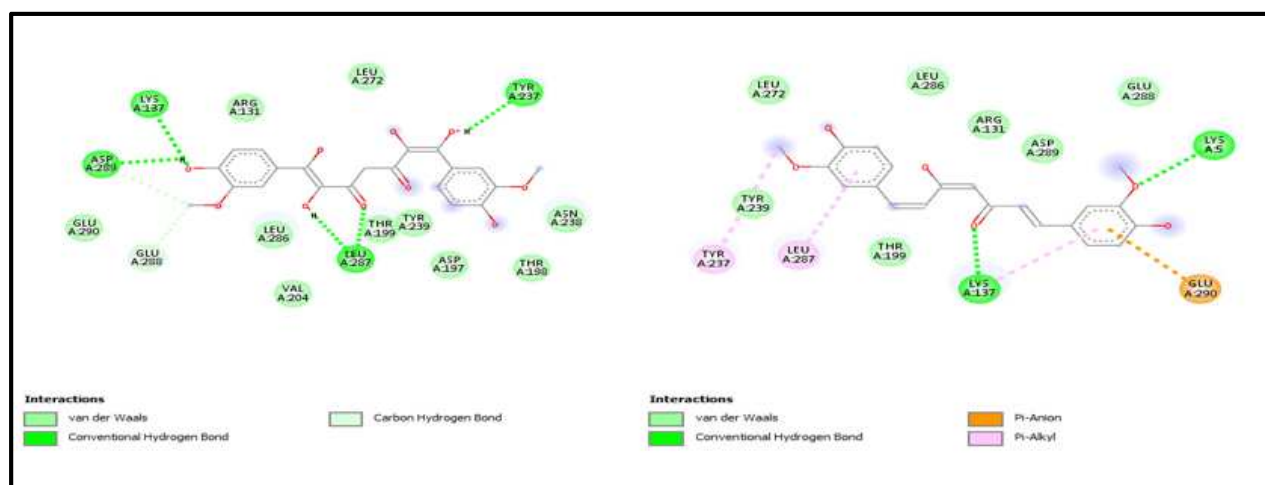


Figure No.2: 2D View of the Binding Conformation of molecule 3 and 4 at the active site of Coronavirus (2019-nCoV) main Protease. (Hydrogen bond interaction)

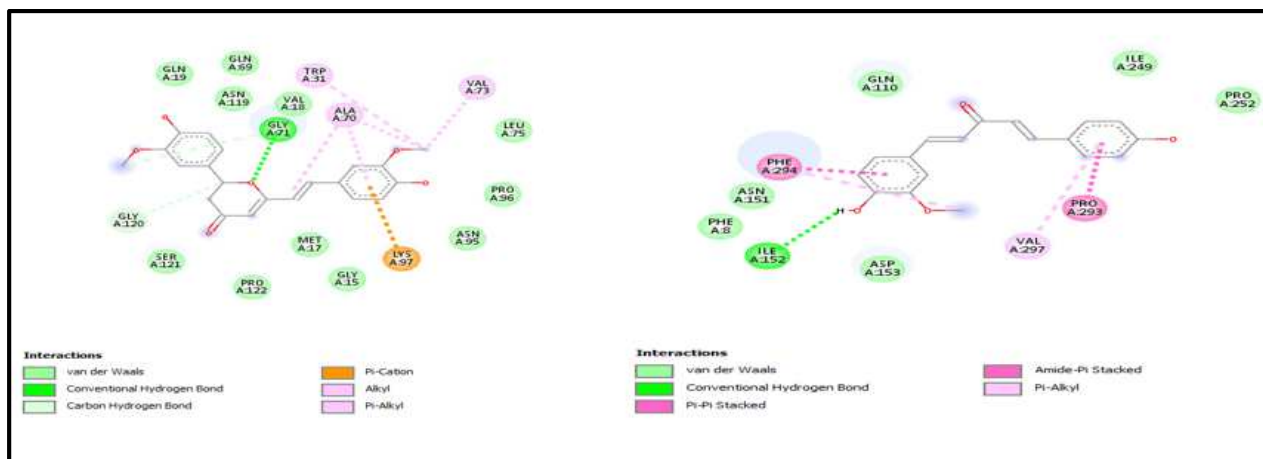


Figure No.3: 2D View of the Binding Conformation of molecule 5 and 6 at the active site of Coronavirus (2019-nCoV) main Protease. (Hydrogen bond interaction)

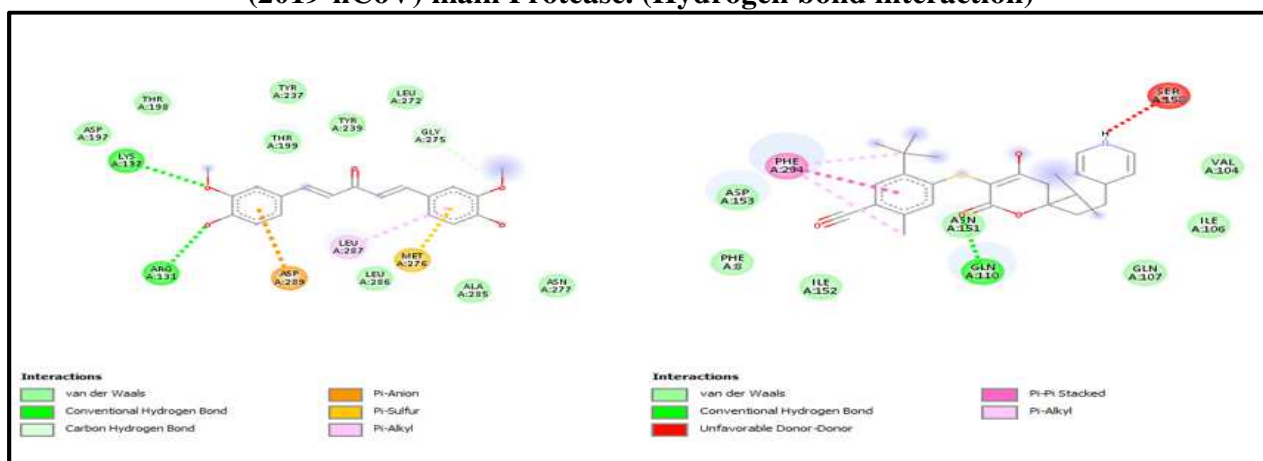


Figure No.4: 2D View of the Binding Conformation of molecule 7 & 8 at the active site of Coronavirus (2019-nCoV) main Protease. (Hydrogen bond interaction)

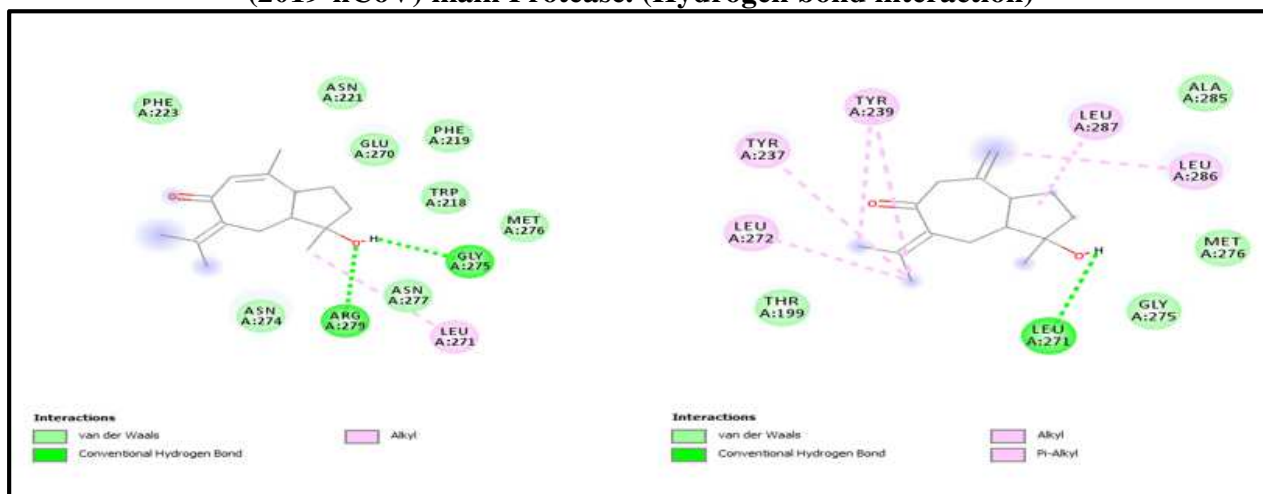


Figure No.5: 2D View of the Binding Conformation of molecule 9 and 10 at the active site of Coronavirus (2019-nCoV) main Protease. (Hydrogen bond interaction)

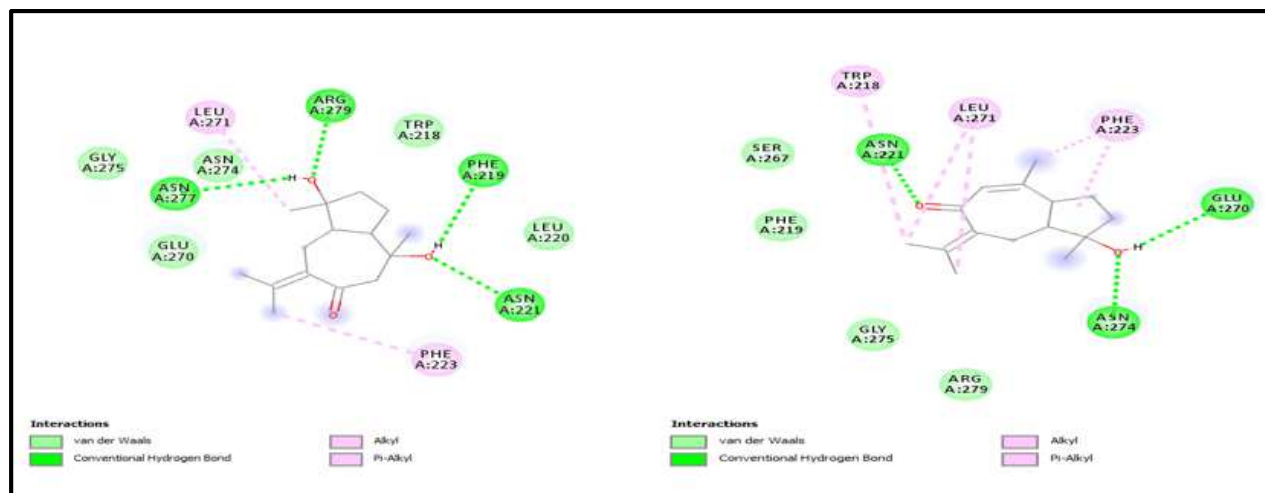


Figure No.6: 2D View of the Binding Conformation of molecule 11 and 12 at the active site of Coronavirus (2019-nCoV) main Protease. (Hydrogen bond interaction)

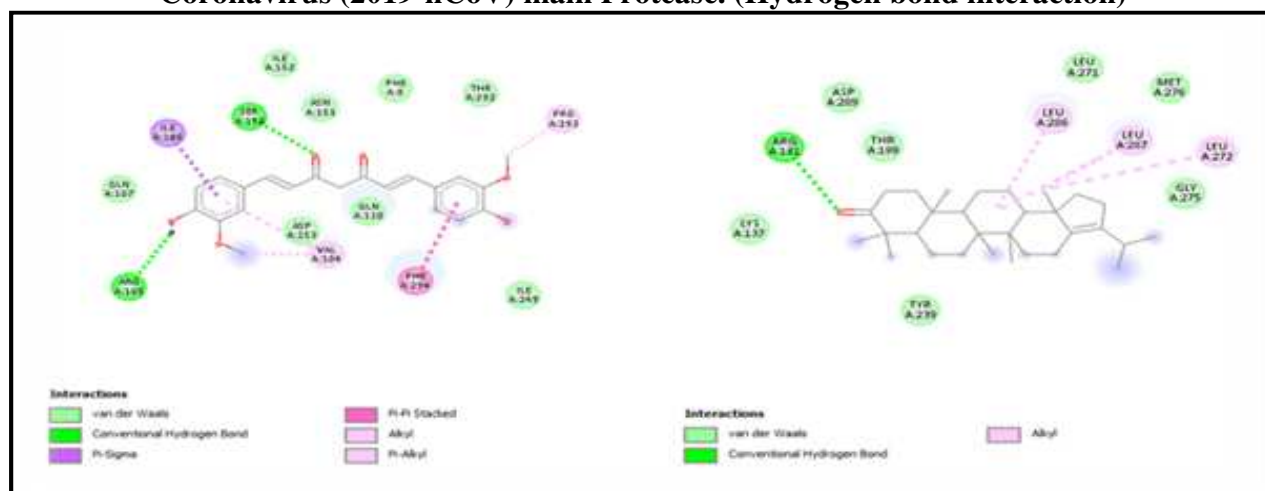


Figure No.7: 2D View of the Binding Conformation of molecule 13 and 14 at the active site of Coronavirus (2019-nCoV) main Protease. (Hydrogen bond interaction)

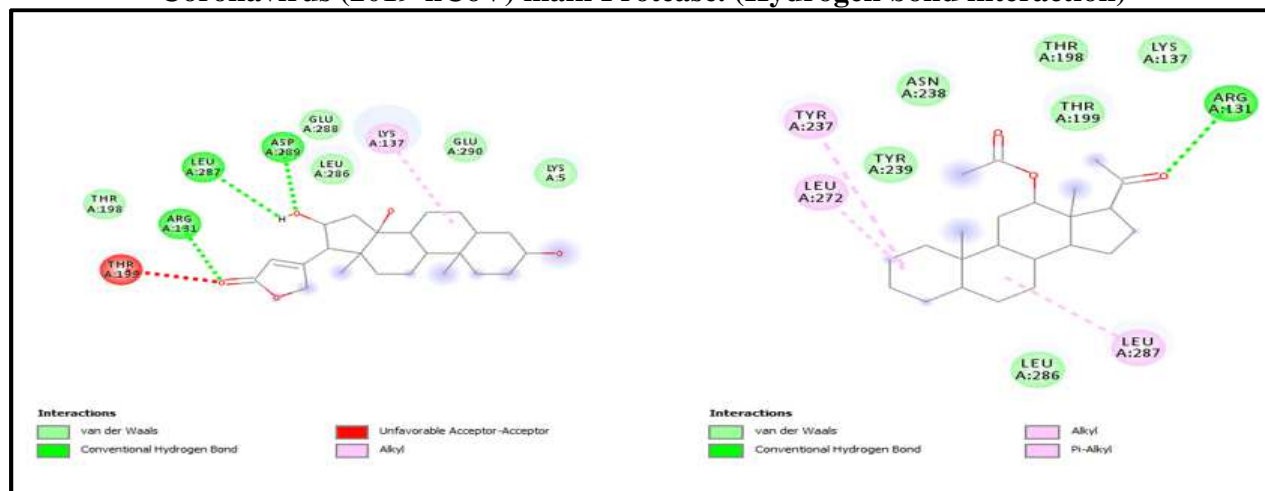


Figure No.8: 2D View of the Binding Conformation of molecule 15 and 16 at the active site of Coronavirus (2019-nCoV) main Protease. (Hydrogen bond interaction)

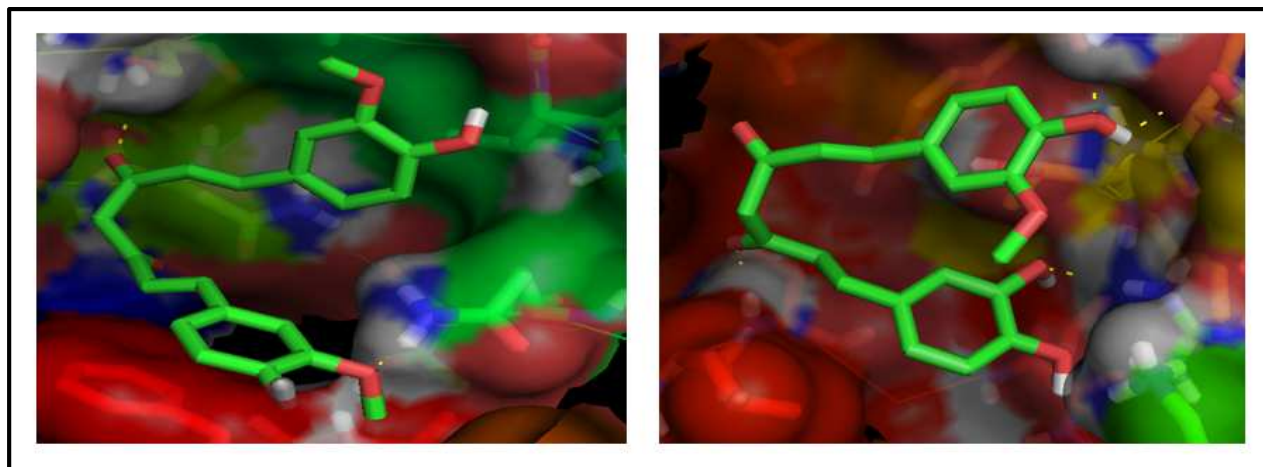


Figure No.9: 3D View of the Binding Conformation of the molecule 1 and 2 at the active site of Coronavirus (2019-nCoV) main Protease

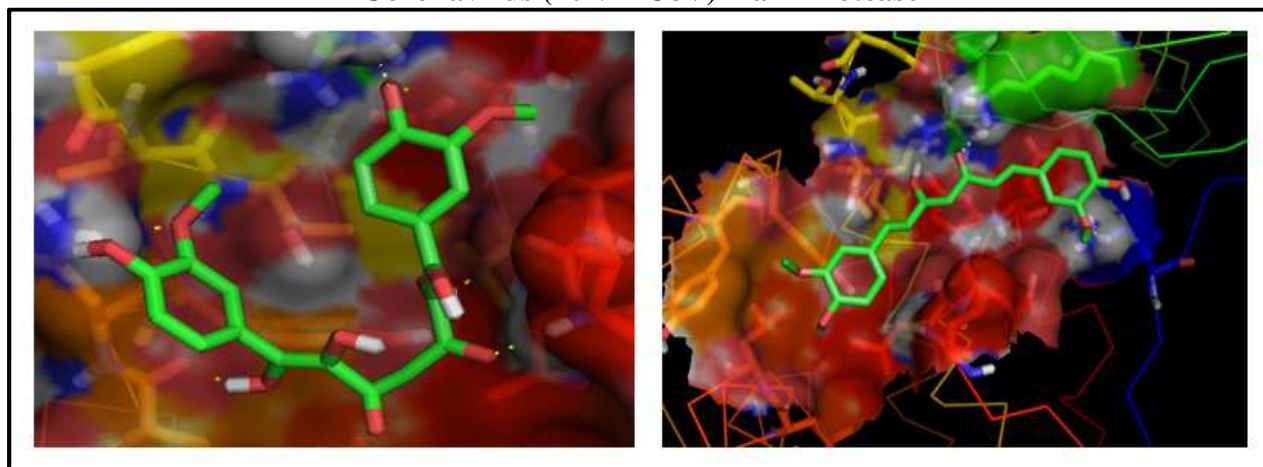


Figure No.10: 3D View of the Binding Conformation of the molecule 3 and 4 at the active site of Coronavirus (2019-nCoV) main Protease

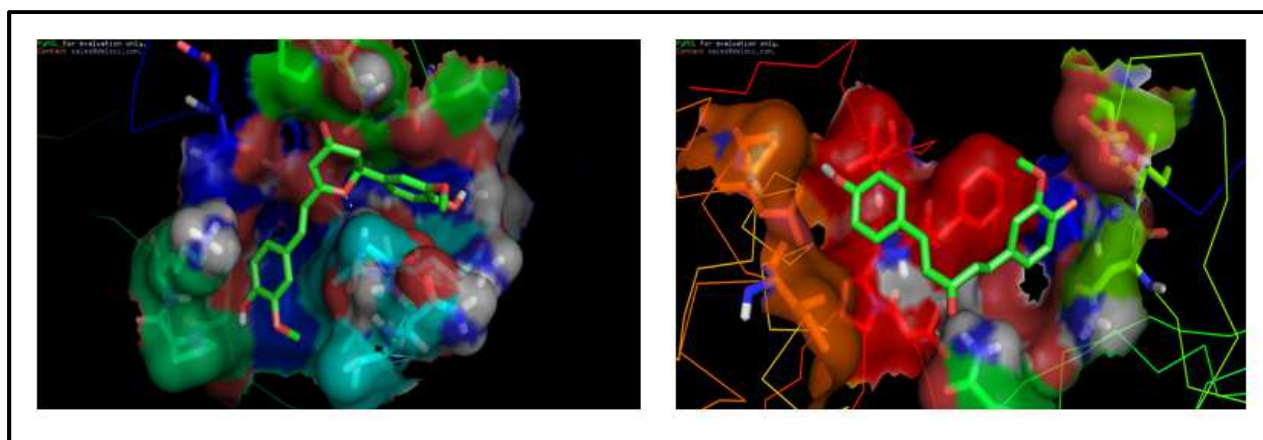


Figure No.11: 3D View of the Binding Conformation of the molecule 5 and 6 at the active site of Coronavirus (2019-nCoV) main Protease

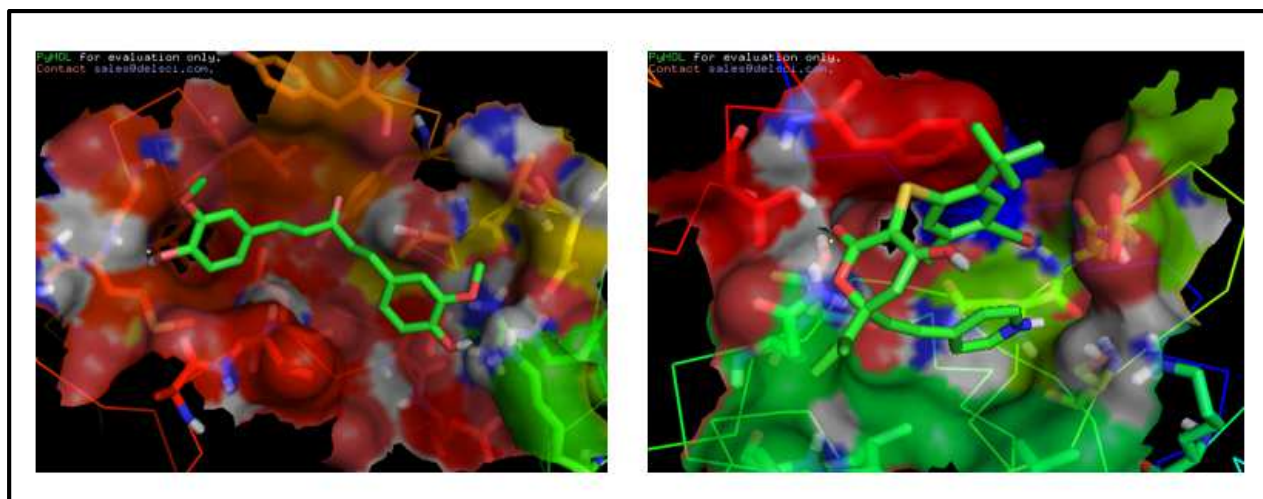


Figure No.12: 3D View of the Binding Conformation of the molecule 7 and 8 at the active site of Coronavirus (2019-nCoV) main Protease

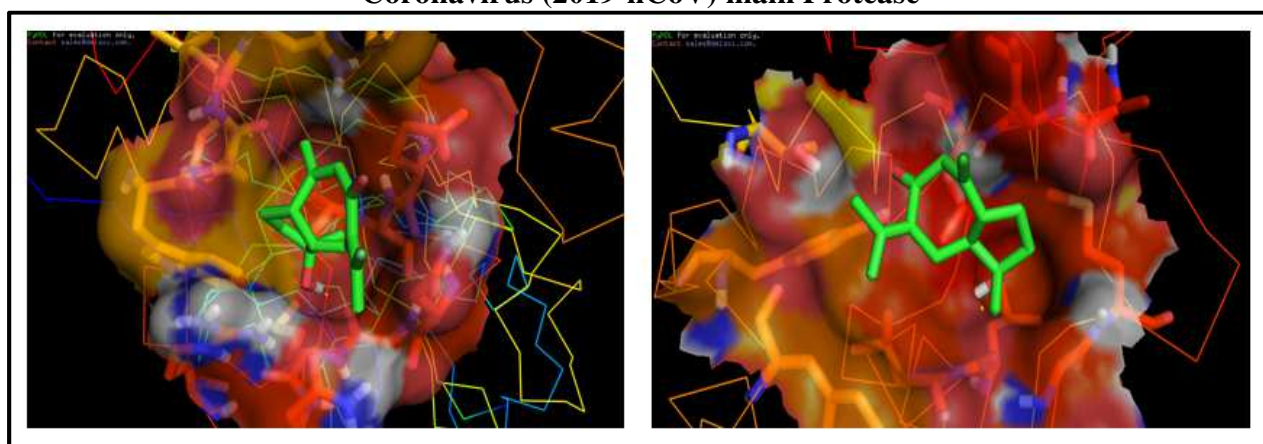


Figure No.13: 3D View of the Binding Conformation of the molecule 9 and 10 at the active site of Coronavirus (2019-nCoV) main Protease

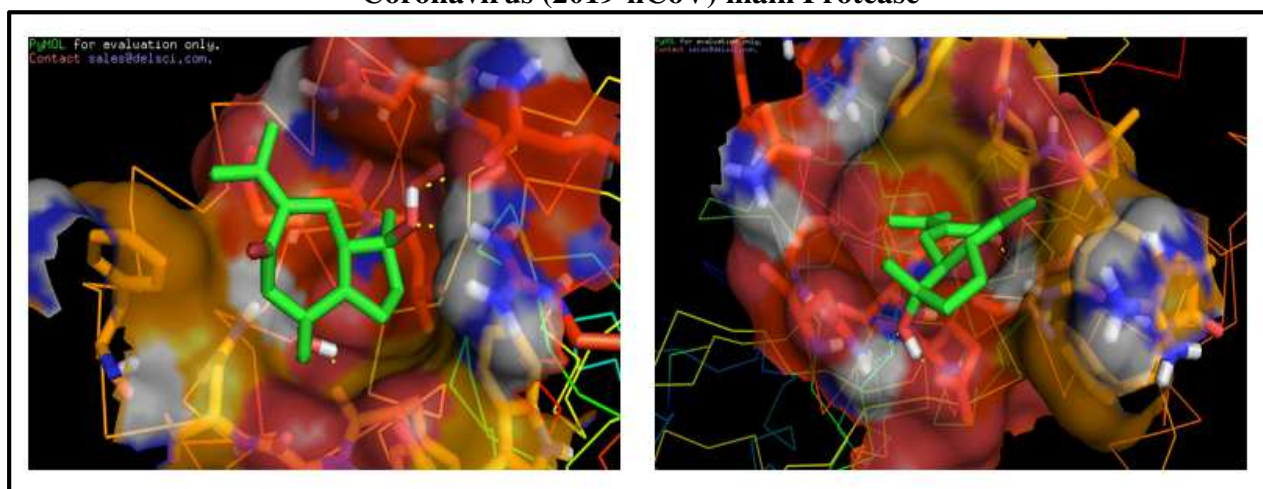


Figure No.14: 3D View of the Binding Conformation of the molecule 11 and 12 at the active site of Coronavirus (2019-nCoV) main Protease

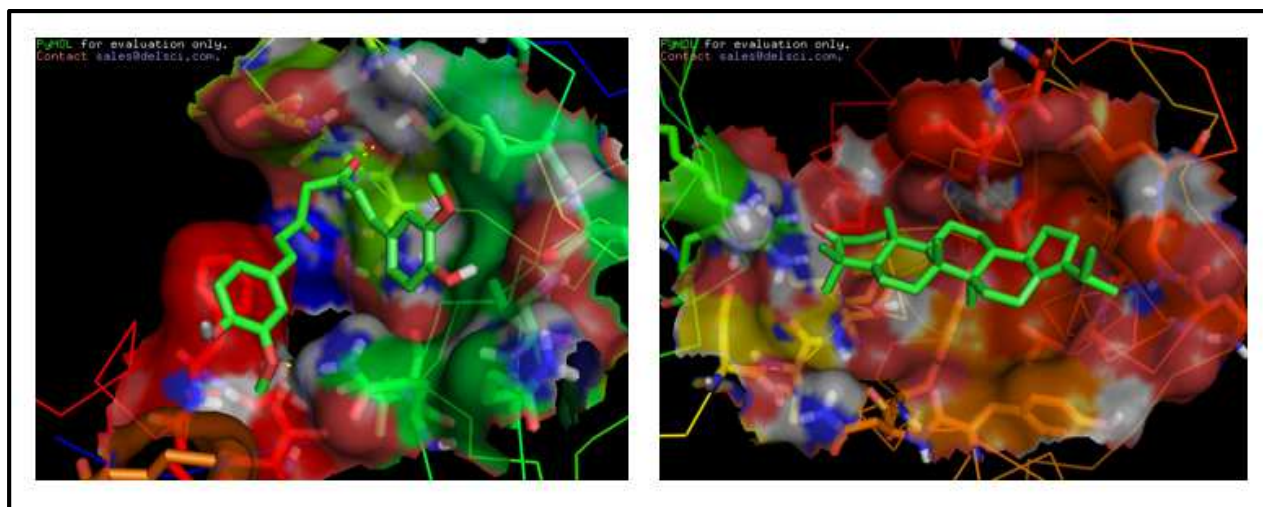


Figure No.15: 3D View of the Binding Conformation of the molecule 13 and 14 at the active site of Coronavirus (2019-nCoV) main Protease

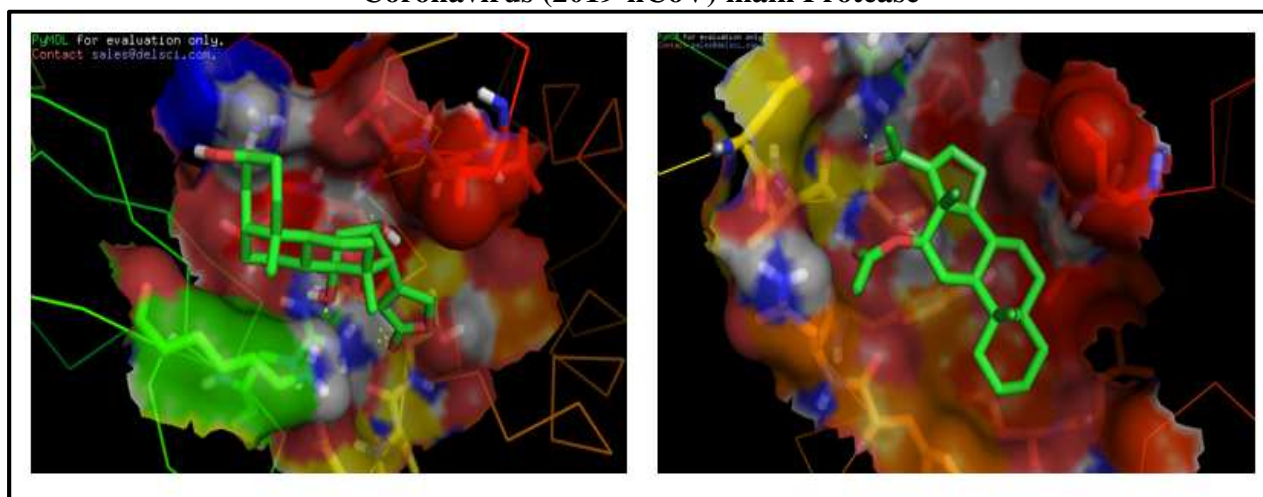


Figure No.16: 3D View of the Binding Conformation of the molecule 15 and 16 at the active site of Coronavirus (2019-nCoV) main Protease

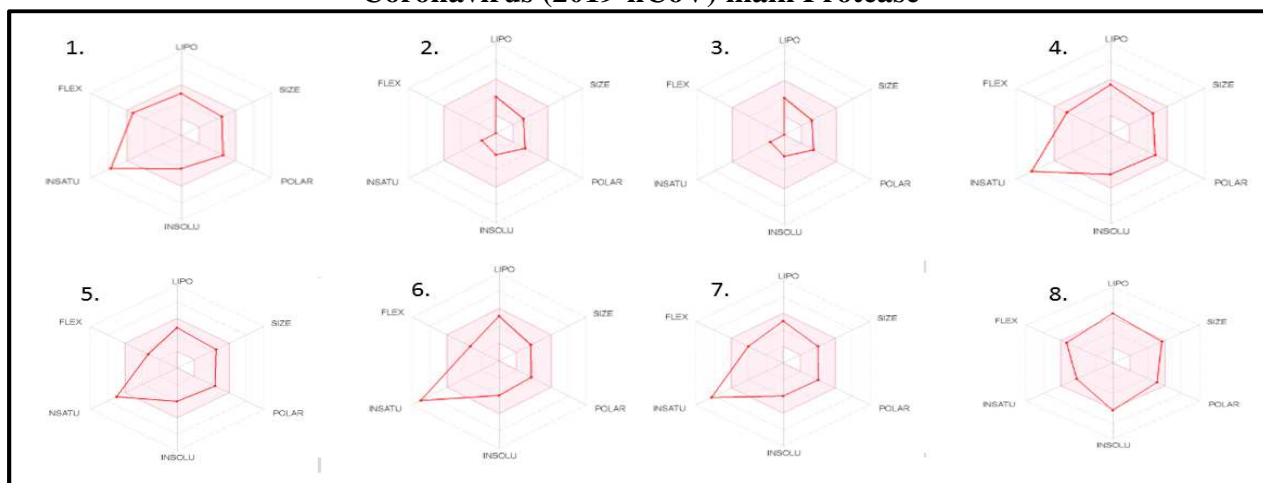


Figure No.17: The Bioavailability rader of the molecule 1 to 8 evaluated using swiss ADME web tool

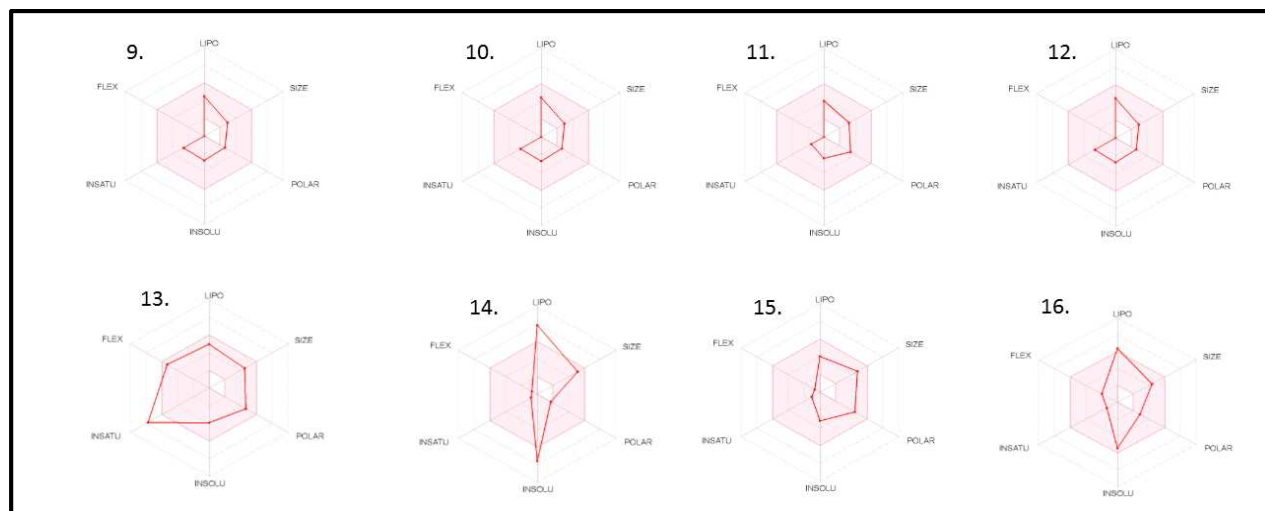


Figure No.18: The Bioavailability rader of the small molecule 9 to 16 evaluated using Swiss ADME web tool

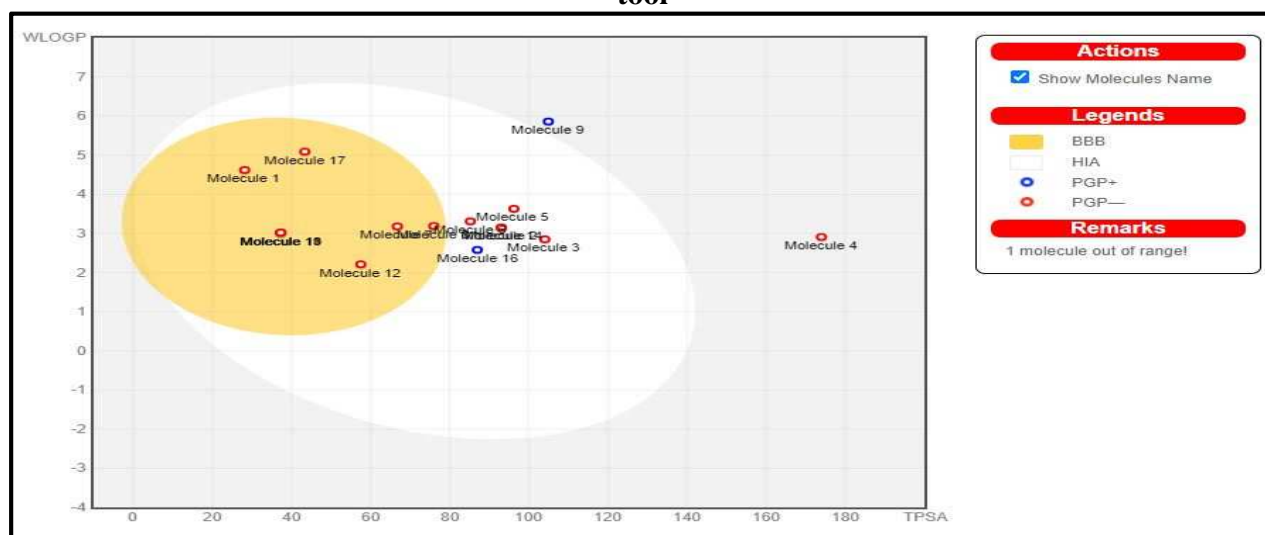


Figure No.19: The Boiled-egg allows for evaluation of passive gastrointestinal absorption (HIA), Brain Penetration (BBB), and p-Glycoprotein activity in presence of molecules. In this figure molecule 1 as a Control and Molecule 2-17 as a top sixteen compounds

CONCLUSION

We reported first time that the derivatives of *Curcuma longa* may play an important role in the inhibition of COVID-19 Mpro through *in silico* study. Approximately 36 derivatives of *Curcuma longa L.* compounds showed the tighter binding affinity at main protease (Mpro) active site. Based on molecular docking and hydrogen bonding, we have observed sixteen compounds among 235 are very interesting for further investigation therefore we propose these molecules against main protease of

SARS-CoV-2. We used the Swiss ADME virtual tools to further evaluate the compounds and demonstrated that all sixteen compounds except Tetrahydrocurcumin, Hopenone I have better “drug-likeness” than control chloroquine. A ‘BOILED egg evaluation’, predicts that all molecules except molecule 4 (Tetrahydrocurcumin) higher gastrointestinal absorption (HIA) than Control and all compounds not effluxed by P-glycoprotein (P-gp). All compounds show good Lipophilicity properties

except two compounds (4''-(4'''-hydroxyphenyl-3-methoxy)-2''-oxo-3''-butenyl-3-(4'-hydroxyphenyl)-propenoate and Hopenone I). All the compounds not substrate of most CYP enzymes of note is the moderate synthetic accessibility of all compounds that provides medicinal chemists with opportunities for synthesis of numerous analogues. The presence of sixteen inhibitor in a single natural product indicated that potential value of COVID-19 virulence and these are the best compounds may be therapeutic value of against SARS-CoV-2. Our selected has been found to show good activity against Mpro but there is need of further pre-clinical and clinical investigations.

ACKNOWLEDGEMENT

We thanks to those who are directly or indirectly helping us to successful in this study. We deeply understand and thanks to our institution Mewar University and respective department are merely acknowledgeable. We highly thankful to use the software's (RBPS Web Portal, BIOVIA Company Discovery studio 2020, and Swiss institute of Bioinformatics).

DECLARATION OF INTEREST

The authors declare no conflict of interest.

BIBLIOGRAPHY

1. Deeks S G, Lewin S R, Ross A L, Ananworanich J, Benkirane M, Cannon P, Kuritzkes D. International AIDS Society global scientific strategy: Towards an HIV cure 2016, *Nature Medicine*, 22(8), 2016, 839-850.
2. Denison M S, Soshilov A A, He G, DeGroot D E and Zhao B. Exactly the same but different: Promiscuity and diversity in the molecular mechanisms of action of the aryl hydrocarbon (dioxin) receptor, *Toxicological Sciences*, 124(1), 2011, 1-22.
3. Petersen E, Hui D, Hamer D H, Blumberg L, Madoff L C, Pollack M, Wasserman S. Li Wenliang, a face to the frontline healthcare worker. The first doctor to notify the emergence of the SARS-CoV-2, (COVID-19), outbreak, *International Journal of Infectious Diseases*, 93, 2020, 205-207.
4. Perlman S. Another decade, another coronavirus, *N Engl J Med*, 382, 2020, 760-762.
5. Hui D S, Azhar E I, Madani T A, Ntoumi F, Kock R, Dar O, Zumla A. The continuing 2019-nCoV epidemic threat of novel coronaviruses to global health-The latest 2019 novel coronavirus outbreak in Wuhan, China, *Int Jour of Inf Di*, 91, 2020, 264-266.
6. Wu A, Peng Y, Huang B, Ding X, Wang X, Niu P, Sheng J. Genome composition and divergence of the novel coronavirus (2019-nCoV) originating in China, *Cell Host and Microbe*, 27(3), 2020, 325-328.
7. Guan W J, Ni Z Y, Hu Y, Liang W H, Ou C Q, He J X, Du B. Clinical characteristics of coronavirus disease 2019 in China, *Ne Eng Jour of Med*, 382(18), 2020, 1708-1720.
8. Zhao S, Lin Q, Ran J, Musa S S, Yang G, Wang W, Wang M H. Preliminary estimation of the basic reproduction number of novel coronavirus (2019-nCoV) in China, from 2019 to 2020: A data-driven analysis in the early phase of the outbreak, *Inter Jour of Infec Dis*, 92, 2020, 214-217.
9. Zou L, Ruan F, Huang M, Liang L, Huang H, Hong Z, Guo Q. SARS-CoV-2 viral load in upper respiratory specimens of infected patients, *New England Journal of Medicine*, 382(12), 2020, 1177-1179.
10. Maurya S K, Maurya A K, Mishra N, Siddique H R. Virtual screening, ADME/T, and binding free energy analysis of anti-viral, anti-protease, and anti-infectious compounds against NSP10/NSP16 methyl transferase and main protease of SARS CoV-2, *Journal of Receptors and Signal Transduction*, 2020, 1-8.
11. Liu W, Zhang Q, Chen J, Xiang R, Song H, Shu S, Wu P. Detection of Covid-19 in children in early January 2020 in Wuhan, China, *New England Journal of Medicine*, 382(14), 2020, 1370-1371.

12. Nick B C, Pandya M C, Lu X, Franke M E, Callahan S M, Hasik E F, Stobart C C. Identification of a critical horseshoe-shaped region in the nsp5 (Mpro, 3CLpro) protease interdomain loop (IDL) of coronavirus mouse hepatitis virus (MHV), *Bio Rxiv*, 2020. 1-33.
13. Bonaca M P, Bauersachs R M, Anand S S, Debus E S, Nehler M R, Patel M R, Hess C N. Rivaroxaban in peripheral artery disease after revascularization, *New England Journal of Medicine*, 382(21), 2020, 1994-2004.
14. Borges Do Nascimento I J, Cacic N, Abdulazeem H M, Von Groote T C, Jayarajah U, Weerasekara I, Carvas Junior N. Novel coronavirus infection (COVID-19) in humans: A scoping review and meta-analysis, *Journal of Clinical Medicine*, 9(4), 2020, 941.
15. Bouhaddou M, Memon D, Meyer B, White K M, Rezelj V V, Marrero M C, Batra J. The global phosphorylation landscape of SARS-CoV-2 infection, *Cell*, 182(3), 2020, 685-712.
16. Nejadi Babadaei M M, Hasan A, Haj Bloukh S, Edis Z, Sharifi M, Kachooei E, Falahati M. The expression level of angiotensin-converting enzyme 2 determine the severity of COVID-19: lung and heart tissue as targets, *Journal of Biomolecular Structure and Dynamics*, 2020, 1-13.
17. Gupta M K, Vemula S, Donde R, Gouda G, Behera L, Vadde R. In-silico approaches to detect inhibitors of the human severe acute respiratory syndrome coronavirus envelope protein ion channel, *Journal of Biomolecular Structure and Dynamics*, 2020, 1-11.
18. Sohrabi C, Alsafi Z, O'Neill N, Khan M, Kerwan A, Al-Jabir A, Agha R. World Health Organization declares global emergency: A review of the 2019 novel coronavirus (COVID-19), *International Journal of Surgery*, 2020, 71-76.
19. Sheahan T P, Sims A C, Leist S R, Schafer A, Won J, Brown A J, Spahn J E. Comparative therapeutic efficacy of remdesivir and combination lopinavir, ritonavir, and interferon beta against MERS-CoV, *Nature Communications*, 11(1), 2020, 1-14.
20. Wang M, Cao R, Zhang L, Yang X, Liu J, Xu M, Xiao G. Remdesivir and chloroquine effectively inhibit the recently emerged novel coronavirus (2019-nCoV) *in vitro*, *Cell Research*, 30(3), 2020, 269-271.
21. Bangalore S, Sharma A, Slotwiner A, Yatskar L, Harari R, Shah B, Chadow H L. ST-segment elevation in patients with COVID-19-a case series, *New England Journal of Medicine*, 382(25), 2020, 2478-2480.
22. Elmezayen A D, Al-Obaidi A, Şahin A T, Yelekci K. Drug repurposing for coronavirus (COVID-19): In silico screening of known drugs against coronavirus 3CL hydrolase and protease enzymes, *Journal of Biomolecular Structure and Dynamics*, 2020, 1-13.
23. Abhishek Kumar Verma, et al. Virtual Screening, Molecular Docking, and ADME/T Analysis of Natural Product Library against Cell Invasion Protein SIPB from *Salmonella enterica serotype typhi*: In Silico Analysis, *Acta Scientific Pharmaceutical Sciences*, 4(8), 2020, 20-30.
24. Trott O, Olson A J. Auto Dock Vina: improving the speed and accuracy of docking with a new scoring function, efficient optimization, and multithreading, *Journal of Computational Chemistry*, 31(2), 2010, 455-461.
25. Verma A K, Maurya S K, Kumar A, Barik M, Yadav V, Umar B, Awal B. Inhibition of multidrug resistance property of *Candida albicans* by natural compounds of *parthenium hysterophorus L.* An In-Silico approach, *Journal of Pharmacognosy and Phytochemistry*, 9(3), 2020, 55-64.
26. Abhishek Kumar Verma and Mayadhar Barik. Natural Compounds against the Main Protease (Mpro) SARS-CoV-2 through In Silico Approach, *Acta Scientific Pharmaceutical Sciences*, 4(8), 2020, 40-41.

27. Lawal M, Verma A K, Umar I A, Gadanya A M, Umar B, Yahaya N, Auwal B. Analysis of new potent anti-diabetic molecules from phytochemicals of pistia strateotes with sglT1 and g6pc proteins of homo sapiens for treatment of diabetes mellitus, An In Silico approach, *IOSR Journal of Pharmacy and Biological Sciences*, 15(4), 2020, 59-73.
28. Delaney J S. ESOL: Estimating aqueous solubility directly from molecular structure, *J Chem Inf Comput Sci*, 44(3), 2004, 1000-1005.
29. Ghose A K, Viswanadhan V N, Wendoloski J J. A knowledge-based approach in designing combinatorial or medicinal chemistry libraries for drug discovery, 1. A qualitative and quantitative characterization of known drug databases, *J Comb Chem*, 1(1), 1999, 55-68.
30. Lagorce D, Sperandio H, Miteva M A et al. FAF-drugs 2: Free ADME/tox filtering tool to assist drug discovery and chemical biology projects, *BMC Bioinformatics*, 9(1), 2008, 396.
31. Ertl P, Rohde B, Selzer P. Fast calculation of molecular polar surface area as a sum of fragment-based contributions and its application to the prediction of drug transport properties, *J Med. Chem*, 43(20), 2000, 3714-3717.
32. Brenk R, Schipani A, James D, Krasowski A, Gilbert I H, Frearson J, et al. Lessons learnt from assembling screening libraries for drug discovery for neglected diseases, *Chem Med Chem*, 3(3), 2008, 435-444.
33. Fagerberg J H, Karlsson E, Ulander J, Hanisch G, Bergstrom C A. Computational prediction of drug solubility in fasted simulated and aspirated human intestinal fluid, *Pharm Res*, 32(2), 2015, 578-589.
34. Maurya S K, Shadab G G H A, Siddique H R. Chemosensitization of Therapy Resistant Tumors: Targeting multiple cell signaling pathways by lupeol, apentacyclic triterpene, *Current Pharmaceutical Design*, 26(4), 2020, 455-465.

Please cite this article in press as: Abhishek Kumar Verma et al. Virtual screening, molecular docking, pharmacokinetic, physicochemical and medicinal properties of potential curcumin derivatives against SARS-CoV-2 main protease (Mpro), *Asian Journal of Pharmaceutical Analysis and Medicinal Chemistry*, 8(4), 2020, 153-179.